

Vito A. Kaminskas
Site Vice President

DTE Energy Company
6400 N. Dixie Highway, Newport, MI 48166
Tel: 734.586.6515 Fax: 734.586.4172
Email: kaminskav@dteenergy.com



10 CFR 54

January 26, 2015
NRC-15-0008

U. S. Nuclear Regulatory Commission
Attention: Document Control Desk
Washington D C 20555-0001

- References:
- 1) Fermi 2
NRC Docket No. 50-341
NRC License No. NPF-43
 - 2) DTE Electric Company Letter to NRC, "Fermi 2 License Renewal Application," NRC-14-0028, dated April 24, 2014 (ML14121A554)
 - 3) NRC Letter, "Requests for Additional Information for the Review of the Fermi 2 License Renewal Application – Set 13 (TAC No. MF4222)," dated December 23, 2014 (ML14351A458)

Subject: Response to NRC Request for Additional Information
for the Review of the Fermi 2 License Renewal Application – Set 13

In Reference 2, DTE Electric Company (DTE) submitted the License Renewal Application (LRA) for Fermi 2. In Reference 3, NRC staff requested additional information regarding the Fermi 2 LRA. Enclosure 1 to this letter provides the DTE response to the request for additional information (RAI). Enclosure 2 to this letter provides the report that was requested in RAI B.1.3-1.

Two new commitments are being made in this submittal. The new commitments are in Item 34, Structures Monitoring, of LRA Table A.4 as indicated in the response to RAI 3.5.2.2.2.1-3.

Should you have any questions or require additional information, please contact Lynne Goodman at 734-586-1205.

I declare under penalty of perjury that the foregoing is true and correct.

Executed on January 26, 2015



Vito A. Kaminskas
Site Vice President
Nuclear Generation

- Enclosures: 1. DTE Response to NRC Request for Additional Information for the
Review of the Fermi 2 License Renewal Application – Set 13
2. 2013 BADGER Test Report

cc: NRC Project Manager
NRC License Renewal Project Manager
NRC Resident Office
Reactor Projects Chief, Branch 5, Region III
Regional Administrator, Region III
Michigan Public Service Commission,
Regulated Energy Division (kindschl@michigan.gov)

**Enclosure 1 to
NRC-15-0008**

**Fermi 2 NRC Docket No. 50-341
Operating License No. NPF-43**

**DTE Response to NRC Request for Additional Information
for the Review of the Fermi 2 License Renewal Application – Set 13**

RAI 3.1.2.1-1

Background

License Renewal Application (LRA) Table 3.1.1 compares the applicant's aging management review (AMR) results for the reactor coolant system against the corresponding entries in "Standard Review Plan for Review of License Renewal Applications for Nuclear Power Plants" (SRP-LR) Table 3.1-1. Item 96 of SRP-LR Table 3.1-1 summarizes the components for which implementation of activities consistent with Generic Aging Lessons Learned (GALL) Report aging management program (AMP) XI.M6, "BWR Control Rod Drive Return Line Nozzle," is an acceptable way to manage the effects of aging. LRA Table 3.1.1 states that there are no AMR results that are comparable with this item.

Issue

LRA Section B.1.5 states that the applicant has an existing BWR Control Rod Drive (CRD) Return Line Nozzle Program that is consistent with GALL Report AMP XI.M6. The components that are within the scope of the applicant's BWR CRD Return Line Nozzle Program are the CRD return line nozzle, the nozzle-to-vessel weld, and the nozzle cap. LRA Table 3.1.2-1 includes an AMR line item for the nozzle cap, but there are no AMR line items in the LRA for the CRD return line nozzle and the associated nozzle-to-vessel weld. Without this information, the LRA does not sufficiently demonstrate that the effects of aging for these components will be adequately managed so that the intended function(s) will be maintained consistent with the current licensing basis (CLB) for the period of extended operation, as required by Title 10 of the Code of Federal Regulations (10 CFR) 54.21(a)(3).

Request

- 1. Provide the AMR results for the CRD return line nozzle and its nozzle-to-vessel weld if these components are within the scope of the BWR CRD Return Line Nozzle Program. Describe how these results compare with SRP-LR Table 3.1-1, item 96.*
- 2. If the CRD return line nozzle and its nozzle-to-vessel weld are not within the scope of the BWR CRD Return Line Nozzle Program, explain how the effects of aging for these components will be adequately managed so that the intended functions will be maintained consistent with the CLB for the period of extended operation.*
- 3. Revise the LRA as appropriate.*

Response:

- 1. The components included in License Renewal Application (LRA) Section B.1.5, BWR CRD Return Line Nozzle Program, were not fully identified in LRA Table 3.1.2-1 line items for the CRD return line nozzle (N9). The Fermi 2 LRA Section B.1.5 BWR CRD Return Line*

Nozzle Program includes the CRD return line nozzle, and its nozzle-to reactor vessel (RV) weld, CRD return line nozzle inconel cap and the inconel weld connecting the CRD return line nozzle to the cap. This is consistent with NUREG-1801 AMP XI.M6.

There is an LRA Table 3.1.2-1 line item for the CRD return line nozzle identified as CRD hydraulic system return (N9) shown with a loss of material aging effect. Line items will be added to Table 3.1.2-1 for the nozzle with the aging effect of cracking and for the nozzle welds with the aging effects of cracking and loss of material. The CRD return line welds will also be added to Table 2.3.1-1. Table 3.1.1, Item 96, will be revised to indicate that the BWR CRD Return Line Nozzle Program manages cracking for the nozzle, cap and welds, but since the materials of the welds and cap are nickel alloy and the mechanism is not cyclic loading, Item 3.1.1-97 is being used for the welds and cap. Additionally, the terminology in LRA Tables 2.3.1-1 and 3.1.2-1 for nozzle N9 is revised for consistency to be CRD return line (N9).

The material is being listed as nickel alloy for the nickel alloy weld and the inconel cap and weld consistent with Section IX.C of NUREG-1801. The low alloy steel nozzle is listed as carbon steel consistent with the convention used throughout the LRA.

2. As described above, the LRA Section B.1.5 BWR CRD Return Line Nozzle Program does include the CRD return line nozzle, and its nozzle-to-vessel weld, CRD return line nozzle cap and nozzle-to-cap weld.
3. The LRA is revised as indicated below.

LRA Revisions:

LRA Tables 2.3.1-1, 3.1.1 (Item 3.1.1-96), and 3.1.2-1 are revised as shown on the following pages. Additions are shown in underline and deletions are shown in strike-through.

**Table 2.3.1-1
 Reactor Vessel
 Components Subject to Aging Management Review**

Component Type	Intended Function
Nozzles <ul style="list-style-type: none"> • Recirc outlet (N1) • Recirc inlet (N2) • Steam (N3) • Core spray (N5) • Space Instrumentation (N6) • Vent (N7) • Jet pump instrument (N8) • CRD hydraulic system return line <u>CRD return line</u> (N9) • Instrumentation (N11, N12) • Seal leak detection (N13) • Instrumentation (N16) • Drain (N15) • Feedwater (N4) 	Pressure boundary
Welds (nozzle to vessel) <ul style="list-style-type: none"> • Instrumentation (N11, N12, N16) 	Pressure boundary
<u>Welds (nozzle to vessel and nozzle to cap)</u> <ul style="list-style-type: none"> • <u>CRD return line (N9)</u> 	<u>Pressure boundary</u>

**Table 3.1.1
 Summary of Aging Management Review Programs for the Reactor Coolant System
 Evaluated in Chapter IV of NUREG-1801**

Table 3.1.1: Reactor Coolant System					
Item Number	Component	Aging Effect/ Mechanism	Aging Management Programs	Further Evaluation Recommended	Discussion
3.1.1-96	Steel (with or without stainless steel cladding) control rod drive return line nozzles exposed to reactor coolant	Cracking due to cyclic loading	Chapter XI.M6, "BWR Control Rod Drive Return Line Nozzle"	No	<u>This item was not used. The Fermi 2 control rod drive return line was cut and capped before initial plant operation. The nozzles have not been exposed to thermal cyclic loading from operation of the return line. However, the BWR CRD Return Line Nozzle Program manages cracking for the control rod drive return line nozzle and nickel alloy cap and nozzle welds. See Item 3.1.1-97 for the nickel alloy cap and nozzle welds.</u>

**Table 3.1.2-1
 Reactor Vessel
 Summary of Aging Management Evaluation**

Table 3.1.2-1: Reactor Vessel								
Component Type	Intended Function	Material	Environment	Aging Effect Requiring Management	Aging Management Programs	NUREG-1801 Item	Table 1 Item	Notes
Nozzles • Recirc outlet (N1) • Recirc inlet (N2) • Steam (N3) • Core spray (N5) • Space Instrumentation (N6) • Vent (N7) • Jet pump instrument (N8) • CRD hydraulic system-return line (N9) • Instrumentation (N11, N12) • Seal leak detection (N13)	Pressure boundary	Carbon steel	Air – indoor (ext)	None	None	--	--	G, 102
			Treated water (int)	Loss of material	Water Chemistry Control – BWR	IV.A1.RP-50	3.1.1-84	A, 101
<u>Nozzles</u> • <u>CRD return line (N9)</u>	<u>Pressure boundary</u>	<u>Carbon steel</u>	<u>Treated water (int)</u>	<u>Cracking</u>	<u>BWR CRD Return Line Nozzle</u>	<u>IV.A1.R-66</u>	<u>3.1.1-96</u>	<u>I</u>
Nozzles • Instrumentation (N16)	Pressure boundary	Carbon steel	Air – indoor (ext)	None	None	--	--	G, 102

Table 3.1.2-1: Reactor Vessel								
Component Type	Intended Function	Material	Environment	Aging Effect Requiring Management	Aging Management Programs	NUREG-1801 Item	Table 1 Item	Notes
Welds (nozzle to vessel) • Instrumentation (N11, N12, N16)	Pressure boundary	Nickel alloy	Treated water (int)	Loss of material	Water Chemistry Control – BWR	IV.A1.RP-157	3.1.1-85	A, 101
Welds (nozzle to vessel and nozzle to cap) • CRD return line (N9)	Pressure boundary	Nickel alloy	Air – indoor (ext)	None	None	IV.E.RP-03	3.1.1-106	A
Welds (nozzle to vessel and nozzle to cap) • CRD return line (N9)	Pressure boundary	Nickel alloy	Treated water (int)	Loss of material	Water Chemistry Control – BWR	IV.A1.RP-157	3.1.1-85	A, 101
Welds (nozzle to vessel and nozzle to cap) • CRD return line (N9)	Pressure boundary	Nickel alloy	Treated water (int)	Cracking	BWR CRD Return Line Nozzle Water Chemistry Control – BWR	IV.A1.R-68	3.1.1-97	E
<i>Safe Ends, Thermal Sleeves, Flanges, Caps, and Welds</i>								

RAI 3.5.1.36-1

Background

Section 54.21(a)(3) of 10 CFR requires the applicant to demonstrate that the effects of aging for structures and components will be adequately managed so that the intended function(s) will be maintained consistent with the CLB for the period of extended operation.

LRA Table 3.5.1, item 3.5.1-36, states that Fermi 2 plant operating experience has not identified fretting or lock up due to mechanical wear for the drywell head and downcomers; that Fermi 2 inspects the drywell head and downcomers per the requirements of American Society of Mechanical Engineers (ASME) Code Section XI; and that the drywell head is a stationary or fixed component and the downcomers are stationary, well-braced components and the spatial distance between connecting components makes it unlikely for fretting and lock up to occur; therefore these aging mechanisms are not applicable.

The staff noted that Section 3.8.2.1.3.6, "Access for Refueling Operations," of the updated final safety analysis report (UFSAR) states that the drywell head is removed during refueling operations and that it is held in place by bolts and is sealed with a double seal.

Issue

Considering the drywell head description in LRA Table 3.5.1, item 3.5.1-36 and the description in Section 3.8.2.1.3.6 of the UFSAR, it is not clear to the staff whether the drywell head is a fixed or removable component and whether the effects of aging on the component has been adequately managed. GALL Report Chapter IX.F states that "wear occurs in parts that experience intermittent relative motion, frequent manipulation, or in clamped joints where relative motion is not intended, but may occur due to a loss of the clamping force." Although fretting or lock up due to mechanical wear has not been identified for the drywell head and downcomers, the relative motion between these surfaces over time may experience fretting or lock up due to wear.

Request

- 1. Clarify whether the drywell head is fixed or removable.*
- 2. If the drywell head is removable, provide an acceptable AMP to demonstrate that the effects of aging on the components will be adequately managed during the period of extended operation. Otherwise provide additional information to justify that fretting or lock up due to mechanical wear does not require aging management.*

Response:

1. The drywell head is a fixed component during plant operation. It is removed for refueling operations as described in the Fermi 2 Updated Final Safety Analysis Report (UFSAR) Section 3.8.2.1.3.6.

The statement "...the drywell head is a stationary or fixed component and..." will be removed from LRA Table 3.5.1, Item 3.5.1-36.

2. NUREG-1801 Section IX.E, Aging Effects, describes fretting as "accelerated deterioration at the interface between contacting surfaces as the result of corrosion and slight oscillatory movement between the two surfaces. In essence, both fretting and lockup are due to mechanical wear." NUREG-1801 Section IX.F, Significant Aging Mechanisms, describes fretting as "...an aging effect due to accelerated deterioration at the interface between contacting surfaces that experience a slight, differential oscillatory movement as the result of corrosion."

There is movement between the drywell head and mating surfaces on the drywell shell only during drywell head removal and re-installation. However, this removal/re-installation cycle does not involve oscillatory movements that could cause fretting and lockup. In addition, while wear can occur in parts that experience intermittent relative motion or frequent manipulation, the removal/re-installation cycle is infrequent (typically once per refueling cycle).

The drywell head bolts are torqued during installation and final torque values are verified in accordance with Fermi 2 procedures. The specific torque values preclude movement between the drywell head and the drywell shell. Thus, fretting and lock up is not an aging effect requiring management for the drywell head surfaces.

LRA Revisions:

LRA Table 3.5.1 (Item 3.5.1-36) is revised as shown on the following page. Additions are shown in underline and deletions are shown in strike-through.

Table 3.5.1: Structures and Component Supports					
Item Number	Component	Aging Effect/ Mechanism	Aging Management Programs	Further Evaluation Recommended	Discussion
3.5.1-36	Steel elements: drywell head; downcomers	Fretting or lockup due to mechanical wear	ISI (IWE)	No	Loss of material is the aging effect caused by mechanical wear. Fermi 2 plant operating experience has not identified fretting or lock up due to mechanical wear for the drywell head and downcomers. Fermi 2 inspects the drywell head and downcomers per the requirements of ASME Section XI. In addition, the drywell head is a stationary or fixed component and the downcomers are stationary, well-braced components and the spatial distance between connecting components makes it unlikely for fretting and lock up to occur.

RAI 3.5.1.93-1

Background

Section 54.21(a)(3) of 10 CFR requires the applicant to demonstrate that the effects of aging for structures and components will be adequately managed so that the intended function(s) will be maintained consistent with the current licensing basis for the period of extended operation. As described in SRP-LR, an applicant may demonstrate compliance with 10 CFR 54.21(a)(3) by referencing the GALL Report and when evaluation of the matter in the GALL Report applies to the plant.

SRP-LR Table 3.5-1, item 93, recommends that galvanized steel, aluminum, or stainless steel support members, welds, bolted connections, and support anchorage exposed to an air outdoor environment be managed for loss of material due to pitting and crevice corrosion by the Structures Monitoring Program. Per the GALL Report, this item relates to supports for cable trays, conduit, HVAC (heating, ventilating, and air conditioning) ducts, tubetrack, instrument tubing, and non-ASME Code piping and components, or to supports for emergency diesel generator, HVAC system components, and other miscellaneous mechanical equipment. LRA Table 3.5.2-4 identifies an AMR result which states that for stainless steel structural bolting exposed to an air outdoor environment, the Inservice Inspection – IWF Program will be used to manage loss of material. This AMR line item cites generic note E, indicating that the material, environment, and aging effect is consistent with the GALL Report but a different AMP is credited. However, the staff notes the SRP-LR Table 3.5-1, item 91, addresses steel support members, welds, bolted connections, and support anchorage for ASME Code Classes 1, 2, 3 and MC supports and recommends the ASME Code Section XI, Subsection IWF Program.

Issue

Based on the information provided in the LRA, it is not clear whether the AMR line item in LRA Table 3.5.2-4 addresses stainless steel structural bolting for ASME Code Section XI, Subsection IWF component supports (e.g. Classes 1, 2, 3, and metal containment piping and components and their associated supports) or non-ASME Code supports as indicated by the reference to GALL Report item III.B2.TP-6. The scope of the Inservice Inspection – IWF Program described in LRA Section B.1.22 appears to be limited to ASME Code Classes 1, 2, 3, and MC piping and component supports.

Request

- 1. For the LRA Table 3.5.2-4 AMR line item associated with SRP-LR Table 3.5-1, item 93, which credits the Inservice Inspection – IWF Program, clarify whether the stainless steel structural bolting is associated with ASME Code Section XI, Subsection IWF components or non-ASME Code component supports.*

- 2. If the structural bolting is for non-ASME Code related component supports, clarify if the stainless steel structural bolting are within the scope of the Inservice Inspection – IWF Program, or propose an AMP that will adequately manage the effects of aging for the stainless steel structural bolting.*

Response:

1. The License Renewal Application (LRA) Table 3.5.2-4 line item for stainless steel structural bolting shown with Standard Review Plan (SRP)-LR Table 3.5-1, item 93, which credits Inservice Inspection – IWF (ISI-IWF) Program was intended for ASME Code Section XI, Subsection IWF components. SRP-LR Table 3.5-1, item 91 was not used because it was for steel, rather than stainless steel, components. In response to this request for additional information, DTE performed further drawing reviews. As a result, the line item for stainless steel structural bolting exposed to air-outdoor environment crediting the ISI-IWF Program will be deleted. No stainless steel bolting within the ISI-IWF Program was identified that is exposed to outdoor air.
2. The line item for stainless steel structural bolting exposed to air-outdoor crediting the ISI-IWF Program is deleted. Line items remain in LRA Table 3.5.2-4 to address carbon steel structural bolting within the ISI-IWF Program and stainless steel structural bolting within the Structures Monitoring Program in the air-outdoor environment.

LRA Revisions:

LRA Table 3.5.2-4 is revised as shown on the following page. Additions are shown in underline and deletions are shown in strike-through.

**Table 3.5.2-4
Bulk Commodities
Summary of Aging Management Evaluation**

Table 3.5.2-4: Bulk Commodities								
Structure and/or Component or Commodity	Intended Function	Material	Environment	Aging Effect Requiring Management	Aging Management Programs	NUREG-1801 Item	Table 1 Item	Notes
Structural bolting	SRE, SSR	Stainless steel	Air—outdoor	Loss of material	ISI-IWF	III.B2.TP-6	3.5.1-93	E

RAI 3.5.2.2.1-2

Background

Section 54.21(a)(3) of 10 CFR requires the applicant to demonstrate that the effects of aging for structures and components will be adequately managed so that the intended function(s) will be maintained consistent with the CLB for the period of extended operation. As described in SRP-LR, an applicant may demonstrate compliance with 10 CFR 54.21(a)(3) by referencing the GALL Report and when evaluation of the matter in the GALL Report applies to the plant.

SRP-LR section 3.5.2.2.1, item 3, addresses cracking and distortion due to increased stress levels from settlement in below-grade inaccessible concrete areas of all groups of structures and states that the existing program relies on structure monitoring programs to manage these aging effects. The SRP-LR also states that some plants may rely on a de-watering system to lower the site ground water level and, if the plant's CLB credits a de-watering system, the GALL Report recommends verification of the continued functionality of the de-watering system during the period of extended operation. LRA Table 3.5.1, item 44, states that Fermi 2 is consistent with the GALL Report recommendation since the concrete in inaccessible areas of all groups of structures exposed to a soil environment will be managed for cracking and distortion due to increased stress levels from settlement by the Structures Monitoring Program. However, the further evaluation, LRA Section 3.5.2.2.1, item 3, states that this aging effect is not applicable to Fermi 2 Groups 1-3 and 5-9 concrete structures since they are founded on bedrock with the exception of the process facilities and yard structures for which this aging effect will be managed by the Structures Monitoring Program. LRA Section 2.4 list all structures associated with Fermi 2 process facilities and yard structures and categorize the turbine building as a different group of structures.

Issue

Based on a review of the information provided in LRA Section 2.4, which states that the turbine building is a nonsafety-related structure, and a review of the information described in Fermi 2 UFSAR Section 3.7.1.5 and Figure 2.4-22, which states that safety related structures and shore barrier are founded on bedrock, the staff was unable to verify whether all portions of the turbine building are founded on bedrock. The staff does not have sufficient information to determine whether the concrete below-grade portion of the turbine building is susceptible to cracking and distortion due to increased stress levels from settlement.

Request

- 1. Describe the foundation type for the Fermi 2 turbine building.*
- 2. If the Fermi 2 turbine building is not founded on bedrock and is susceptible to cracking and distortion due to increased stress levels from settlement, state how this aging effect will be adequately managed for the period of extended operation. Otherwise provide additional*

information to justify that cracking and distortion due to increased stress levels from settlement does not require aging management.

Response:

1. Site drawings and calculations confirm that the Fermi 2 turbine building has a mat foundation founded on bedrock. The turbine building foundation is separate and independent from the turbine pedestal as stated in License Renewal Application (LRA) Section 2.4.3. The turbine pedestal is also founded on bedrock.
2. Not applicable since the turbine building is founded on bedrock.

LRA Revisions:

None.

RAI 3.5.2.2.1-3

Background

Section 54.21(a)(3) of 10 CFR requires the applicant to demonstrate that the effects of aging for structures and components will be adequately managed so that the intended function(s) will be maintained consistent with the current licensing basis for the period of extended operation. SRP-LR Section 3.5.2.2.2.1, item 4, addresses increase in porosity and permeability, and loss of strength due to leaching of calcium hydroxide and carbonation in below-grade inaccessible concrete areas of Groups 1-5 and 7-9 structures and states that the GALL Report recommends further evaluation if leaching is observed in accessible areas that impacts the intended functions of the concrete structure. The SRP-LR also states that a plant-specific AMP is not required for the reinforced concrete exposed to flowing water if (1) there is evidence in the accessible areas that the flowing water has not caused leaching of calcium hydroxide and carbonation or (2) evaluation determined that the observed leaching of calcium hydroxide and carbonation in accessible areas has no impact on the intended function of the concrete structure.

LRA Table 3.5.1, item 47, states that this item is not applicable since Fermi 2 Category I structures are founded on bedrock, do not have water flowing underneath the foundation, and leaching has not been observed on accessible portions of Fermi 2 accessible concrete areas. The further evaluation, LRA Section 3.5.2.2.2.1, item 4, also states that this aging effect is not applicable for concrete of Fermi 2 Groups 1-5 and 7-9 concrete structures since structures are not subject to the flowing water environment necessary for this aging effect to occur. However, during the onsite AMP audit, the staff observed indications of concrete leaching in the floor and walls of the turbine building basement, and identified operating experience associated with groundwater in-leakage and leaching issues in the reactor building, residual heat removal (RHR) complex, and manholes.

Issue

The statement that "leaching has not been observed on accessible portions of Fermi 2 accessible concrete areas" in LRA Table 3.5.1, item 47, is not consistent with the applicant's operating experience reviewed by the staff during the onsite AMP audit.

LRA Section 3.5.2.2.2.1, item 4, does not discuss operating experience related to the leaching observed in accessible areas nor discuss any evaluation of how the observed leaching of calcium hydroxide and carbonation in accessible areas has no impact on the intended function of the concrete structure in order to address the further evaluation criteria.

Request

1. Provide a summary of operating experience regarding leaching of calcium hydroxide and carbonation in accessible areas of Fermi 2 Groups 1-5 and 7-9 concrete structures.

2. *State if an evaluation to determine the impact of the observed leaching of calcium hydroxide and carbonation on the intended function of the concrete structure has been performed and describe the results.*
3. *If no evaluation has been performed for the observed leaching of calcium hydroxide and carbonation in accessible areas, state and describe how this aging effect will be adequately managed for inaccessible areas.*

Response:

1. The following is a summary of water in-leakage events documented by the Fermi 2 Corrective Action Program (CAP) regarding potential leaching of calcium hydroxide and carbonation in accessible areas of Fermi 2 Groups 1-5 and 7-9 concrete structures:
 - **Condition Assessment Resolution Document (CARD) 04-22867** – Water was observed leaking through the west wall of the reactor building and forming a puddle on the floor of the torus room near the 170° azimuth. The leak was categorized as a “small ground water leak”, and there were no indications of discoloration, crystallization or mineral deposits noted in the CARD.
 - **CARD 07-23339** – Water in-leakage, staining and build-up of corrosion products was observed on inside surfaces of manhole #16955, located in the turbine building basement pipe tunnel east of col. row ‘S’.
 - **CARD 09-26756** – Honeycomb, hairline cracking and crystallization/mineral deposits were observed on the north wall of the residual heat removal (RHR) complex. There was a question as to whether the cracking was caused by alkali-silica reaction (ASR). The disposition of this CARD included procuring the services of an expert in the fields of forensic investigation and concrete restoration who determined that ASR was not the cause of this cracking.
 - **CARDs 10-22385 & 08-22565** – These CARDs document cracks, water in-leakage and white mineral deposits in walls of the auxiliary building basement, control air compressor (CAC) room (10-22385) and in walls of the torus room in the reactor building basement (08-22565).
 - **CARDs 12-27792 & 08-20063** – These CARDs document cracks, water in-leakage and white mineral deposits in walls of the reactor building sub-basement and basement quads and torus room, and walls of the auxiliary building sub-basement high pressure coolant injection (HPCI) room and basement control rod drive (CRD) pump room (12-27792) and various other locations (08-20063).
 - **CARD 14-26270** – This CARD documents cracks, water in-leakage and white mineral deposits in concrete elements in several locations in the turbine building basement. This CARD was initiated as a result of the 2014 Structures Monitoring Program walkdowns.
2. The mineral deposits associated with the in-leakage discussed above have generally been characterized as efflorescence. To confirm that these deposits are not the result of leaching of calcium hydroxide and carbonation that could impact the intended function(s) of the concrete

structures, the following testing and evaluation will be performed prior to the period of extended operation (PEO).

- a. DTE will test available water/mineral deposit samples from the areas discussed in Item 1 for mineral and iron content to assess the effect of the water in-leakage on the reinforced concrete elements involved.
 - b. The results of the testing and Structures Monitoring Program inspections will be used to determine corrective actions per the Corrective Action Program. Possible corrective actions include, but are not limited to, more frequent inspections, sampling and analysis of the in-leakage water for mineral and iron content, testing core bore samples, and evaluation of the affected area using evaluation and acceptance criteria of ACI 349.3R.
 - c. The testing and evaluation activities will commence in 2015 through the Corrective Action Program, and will be completed prior to the PEO.
3. As discussed in the response to Item 2 above, to confirm that the conditions described in the response to Item 1 are not the result of leaching of calcium hydroxide and carbonation that could impact intended function of the concrete structures, further testing and evaluation will be performed prior to PEO. Similar testing will also be performed on samples for future observances of the same nature, to determine whether these concrete elements in accessible areas are experiencing leaching of calcium hydroxide and carbonation. Based on the testing results, further evaluations will be performed to determine whether the observed conditions in the accessible areas have any impact on the intended functions of the concrete elements. Also, in accordance with the SRP-LR, if the observed conditions in accessible areas are found to impact the intended functions of the concrete elements in question, then a similar corrective action plan will be developed for testing and evaluation of concrete elements in inaccessible areas, as per the enhancement included in LRA Section B.1.42. The following additional enhancement to the LRA Section B.1.42 program provides for the management of this potential aging effect:
- a) Revise plant procedures to include testing and evaluation of water/mineral deposits where in-leakage is observed in concrete elements. Testing and evaluation will determine whether leaching of calcium hydroxide and carbonation are occurring that could impact the intended function(s) of the concrete structure.

This enhancement will be implemented prior to PEO.

LRA Revisions:

LRA Sections A.1.42, A.4, and B.1.42 are revised as shown on the following pages. Additions are shown in underline and deletions are shown in strike-through.

A.1.42 Structures Monitoring Program

The Structures Monitoring Program will be enhanced as follows.

- Revise plant procedures to prescribe quantitative acceptance criteria based on the quantitative acceptance criteria of ACI 349.3R and information provided in industry codes, standards, and guidelines including ACI 318, ANSI/ASCE 11, and relevant AISC specifications. Industry and plant-specific operating experience will also be considered in the development of the acceptance criteria.
- Revise Structures Monitoring Program procedures to include testing and evaluation of water/mineral deposits where in-leakage is observed in concrete elements. Testing and evaluation will determine whether leaching of calcium hydroxide and carbonation are occurring that could impact the intended function(s) of the concrete structure.
- The following testing and evaluation will be performed prior to the period of extended operation to confirm that previously identified conditions are not the result of leaching of calcium hydroxide and carbonation that could impact the intended function(s) of the concrete structure.
 - ▶ Available water/mineral deposit samples will be tested for mineral and iron content to assess the effect of the water in-leakage on the reinforced concrete elements involved.
 - ▶ The results of the testing and Structures Monitoring Program inspections will be used to determine corrective actions per the Corrective Action Program. Possible corrective actions include, but are not limited to, more frequent inspections, sampling and analysis of the in-leakage water for mineral and iron content, testing core bore samples, and evaluation of the affected area using evaluation and acceptance criteria of ACI 349.3R-02 or later.

A.4 LICENSE RENEWAL COMMITMENT LIST

No.	Program or Activity	Commitment	Implementation Schedule	Source
34	Structures Monitoring	<p>Enhance Structures Monitoring Program as follows:</p> <p><u>m. Revise Structures Monitoring Program procedures to include testing and evaluation of water/mineral deposits where in-leakage is observed in concrete elements. Testing and evaluation will determine whether leaching of calcium hydroxide and carbonation are occurring that could impact the intended function(s) of the concrete structure.</u></p> <p><u>n. The following testing and evaluation will be performed prior to the period of extended operation to confirm that previously identified conditions are not the result of leaching of calcium hydroxide and carbonation that could impact the intended function(s) of the concrete structure.</u></p> <ul style="list-style-type: none"> • <u>Available water/mineral deposit samples will be tested for mineral and iron content to assess the effect of the water in-leakage on the reinforced concrete elements involved.</u> • <u>The results of the testing and Structures Monitoring Program inspections will be used to determine corrective actions per the Corrective Action Program. Possible corrective actions include, but are not limited to, more frequent inspections, sampling and analysis of the in-leakage water for mineral and iron content, testing core bore samples, and evaluation of the affected area using evaluation and acceptance criteria of ACI 349.3R-02 or later.</u> 	<p>Prior to September 20, 2024. Testing and evaluation for possible leaching in previously identified conditions will commence in 2015.</p>	A.1.42

B.1.42 STRUCTURES MONITORING

Enhancements

Element Affected	Enhancement
<p><u>3. Parameters Monitored or Inspected</u> <u>4. Detection of Aging Effects</u></p>	<p><u>Revise Structures Monitoring Program procedures to include testing and evaluation of water/mineral deposits where in-leakage is observed in concrete elements. Testing and evaluation will determine whether leaching of calcium hydroxide and carbonation are occurring that could impact the intended function(s) of the concrete structure.</u></p>
<p><u>6. Acceptance Criteria</u></p>	<p><u>Revise plant procedures to prescribe quantitative acceptance criteria based on the quantitative acceptance criteria of ACI 349.3R and information provided in industry codes, standards, and guidelines including ACI 318, ANSI/ASCE 11 and relevant AISC specifications. Industry and plant-specific operating experience will also be considered in the development of the acceptance criteria.</u></p>
<p><u>4. Detection of Aging Effects</u> <u>7. Corrective Actions</u></p>	<p><u>The following testing and evaluation will be performed prior to the period of extended operation to confirm that previously identified conditions are not the result of leaching of calcium hydroxide and carbonation that could impact the intended function(s) of the concrete structure.</u></p> <ul style="list-style-type: none"> • <u>Available water/mineral deposit samples will be tested for mineral and iron content to assess the effect of the water in-leakage on the reinforced concrete elements involved.</u> • <u>The results of the testing and Structures Monitoring Program inspections will be used to determine corrective actions per the Corrective Action Program. Possible corrective actions include, but are not limited to, more frequent inspections, sampling and analysis of the in-leakage water for mineral and iron content, testing core bore samples, and evaluation of the affected area using evaluation and acceptance criteria of ACI 349.3R-02 or later.</u>

RAI B.1.3-1

Background

During the Fermi 2 onsite AMP audit, the applicant stated that three Boraflex panels were taken out of service because their Boron-10 areal density measurement test results did not meet the acceptance criteria. The measurement test results are found in the 2013 Fermi 2 BADGER test report, which summarizes the Boraflex test campaign conducted in 2013.

Issue

The report provides information on the condition of the Boraflex material in the spent fuel pool and by extension the effectiveness of the Boraflex Monitoring Program. The staff reviewed the 2013 BADGER test report briefly during its onsite audit; however, more information is needed to complete its review and reach a conclusion on the adequacy of the Boraflex Monitoring Program to manage the effects of aging.

Request

Please provide the 2013 BADGER test report to the staff so a more detailed review can be performed to assess the condition of the Boraflex material and the effectiveness of the Boraflex Monitoring Program.

Response:

The 2013 BADGER test report is provided in Enclosure 2 of this letter.

LRA Revisions:

None.

**Enclosure 2 to
NRC-15-0008**

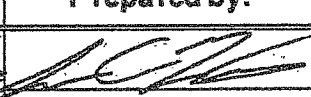
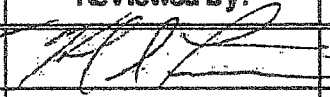
**Fermi 2 NRC Docket No. 50-341
Operating License No. NPF-43**

2013 BADGER Test Report

BADGER Test Campaign at Enrico Fermi Power Plant 2

Prepared by:
NETCO, a business unit of Curtiss-Wright Flow Control Corp.
731 Grant Ave
Lake Katrine, New York 12449

Prepared for:
DTE Energy
under
Purchase Order No. 4700406967

Rev:	Date:	Prepared by:	Reviewed by:	Approved by:
0	2/14/08			L. P. Mariani

BADGER Applicability Statement

This report was prepared by NETCO, a Business Unit of Curtiss-Wright Flow Control. The report was developed under the requirements of the NETCO quality assurance program in order that the technical quality could be verifiably controlled. The BADGER device is calibrated using plant design basis fuel cell configurations and plant design basis panel areal densities. BADGER data is processed using controlled spreadsheet software, which is currently classified by NETCO, as per the requirements of ASME-NQA1, as augmented quality software since it cannot be fully benchmarked. This circumstance hinders the ability to precisely quantify all of the biases, tolerances and uncertainties inherent in the methodology described herein.

Consequently, when drawing conclusions concerning the current and eventual status of neutron absorber panels, the end user of this report is obliged to conservatively utilize all available plant-specific information (i.e. BADGER test results, surveillance coupon reports, spent fuel pool chemistry as well as other applicable plant conditions).

Abstract

Boraflex is a neutron absorber material used for criticality control in some spent fuel racks. Premature deterioration of this material, via radiation induced shrinkage and slow dissolution of the residual matrix, has been observed in some racks. The Boron-10 Areal Density Gage for Evaluating Racks (BADGER) was developed by Northeast Technology Corp. (NETCO) for the Electric Power Research Institute (EPRI). BADGER is a device that allows the in-situ measurement of the boron-10 areal density of the neutron absorber material installed in spent fuel racks for the purpose of reactivity control. This report describes the BADGER test conducted at DTE Energy's Fermi 2 Nuclear Station October 7 – 16, 2013.

The following report provides an overview of the BADGER system, the test data from the Fermi 2 campaign, an evaluation of that data including the measured areal densities and NETCO's conclusions with respect to the condition of the Boraflex in the Fermi 2 spent fuel racks.

BADGER testing indicated that the average areal density of the tested panels is approximately the same as the as-built areal density values.

Some localized Boraflex deterioration has been noted which may impact the criticality analysis of record and future fuel management schemes.

The RACKLIFE model provides a means for forecasting the rate at which each panel of Boraflex accumulates gamma exposure. Therefore, RACKLIFE provides the means to help evaluate and implement rack management strategies and to mitigate the effects of Boraflex degradation ^[6].

Table of Contents

BADGER APPLICABILITY STATEMENT	II
ABSTRACT	III
TABLE OF CONTENTS.....	IV
LIST OF TABLES	V
LIST OF FIGURES.....	VI
1.0 INTRODUCTION	1
2.0 OVERVIEW OF THE BADGER SYSTEM.....	2
2.1 BADGER EQUIPMENT DESCRIPTION.....	2
2.2 TYPICAL OPERATION OF BADGER.....	3
3.0 SCOPE OF THE TESTING AT FERMI 2	7
3.1 SPENT FUEL RACK DESCRIPTION.....	7
3.2 BORAFLEX PANELS SELECTED FOR TESTING	8
4.0 BADGER TEST RESULTS.....	14
4.1 PANEL DETECTOR TRACES	14
4.2 PANEL AVERAGE AREAL DENSITY	15
4.3 GAPS, CRACKS, AND OTHER ANOMALIES	17
5.0 CONCLUSIONS	31
5.1 TEST RESULTS.....	31
5.2 RECOMMENDATIONS.....	32
6.0 REFERENCES.....	33

APPENDIX A: BADGER Panel Traces for Tested Panels

List of Tables

Table		Page
3-1	RACKLIFE-Estimated Dose for Fermi 2 Boraflex Panels Tested	9
4-1	Fermi 2 Results for All Tested Boraflex Panels	23

List of Figures

Figure	Page
2-1 Typical Axial Cross Section of the Source and Detector Heads in Fuel Rack Cells	5
2-2 Lateral Cross Section of the Source and Detector Heads	6
3-1 Fuel Rack Boraflex Configurations	10
3-2 Isometric View of a Cruciform Element	11
3-3 A 3x3 Array of Fuel Cells	12
3-4 Distribution of (Estimated) Panel Dose in the Fermi 2 Spent Fuel Pool	13
4-1 Panel Traces for Panel B33 South	19
4-2 Panel Traces for Panel KK57 West. Features a Large Gap at 140"	20
4-3 Panel Traces for Panel QQ64 South. Features a Local Dissolution at ~80"	21
4-4 Panel Traces for Panel JJ56 South. Features a Large Gap at 130" and Local Dissolution from 0"-40"	22
4-5 Distribution of Measured Areal Density Values Ranked by Panel Name for each rack location	26
4-6 Distribution of Measured Areal Density Values Ranked by Areal Density	27
4-7 Distribution of Measured Areal Density (AD) Values versus the Estimated Dose as Predicted by RACKLIFE	28
4-8 Distribution of the Cumulative Gap Size Observed on a Panel versus the Estimated Accumulated Dose as Predicted by RACKLIFE	29
4-9 Histogram of the Number of Panels that have X" of Cumulative Gap Size	30

1.0 INTRODUCTION

Boraflex is a neutron absorber material used for criticality control in some spent fuel racks. Premature deterioration of this material, via radiation induced shrinkage and slow dissolution of the residual matrix, has been observed in some racks.^[1,2,3] The Boron-10 Areal Density Gauge for Evaluating Racks (BADGER) was developed by Northeast Technology Corp. (NETCO) for the Electric Power Research Institute (EPRI) under research project WO-3907-01.^[4,5] BADGER is a device which allows the in-situ measurement of the boron-10 areal density (¹⁰B density expressed as grams ¹⁰B/cm²) of the neutron absorber material installed in spent fuel racks for the purpose of reactivity control. The development of BADGER was prompted by the observed in-service deterioration of Boraflex, as noted above. This report describes the BADGER test conducted at DTE Energy's Fermi 2 Nuclear Station October 7 – October 16, 2013. The testing was performed according to NETCO's Special Engineering Procedure: SEP-300010-05, Rev 0^[7].

To improve system performance and reliability, NETCO has subjected the BADGER system to a detailed redesign. Many of the NETCO-identified elements addressed in the redesign were noted by the Nuclear Regulatory Commission (NRC) commissioned report "Boraflex, RACKLIFE, and BADGER" (ML12216A307). The BADGER upgrades include: a more reliable, consistent, and stronger neutron pulse signal achieved with upgraded cables, upgraded pre-amplifiers, and well-sealed detector housings. NETCO also increased the stability of the probe heads to reduce uncertainty in head alignment. Additional detector shielding was added to filter out detected neutrons that were not transmitted through the absorber panel. Drive system and software enhancements add a level of reliability and a finer level of control. All of these developments were subjected to testing at NETCO's test facility before use in a commercial environment, as required by the NETCO design control process.

Fermi 2's RACKLIFE model provided a means to identify those storage cells and specific Boraflex panels that had been subjected to the most severe service histories in terms of integrated gamma exposure and, potentially, the greatest boron carbide loss. A sample population of the panels was selected, which included some of the highest exposed panels (1.67×10^{10} rads), as well as a series of panels which had accumulated a spectrum of exposures ranging from lower dose panels up to the highest dose panels. Sixty (60) of these panels were scanned from the Joseph Oat manufactured spent fuel racks. The RACKLIFE model provides a means for forecasting the rate at which each panel of Boraflex accumulates gamma exposure. Therefore the model provides the means for evaluating and implementing rack management strategies to help mitigate the effects of Boraflex degradation.

2.0 OVERVIEW OF THE BADGER SYSTEM

2.1 *BADGER Equipment Description*

Figure 2-1 schematically depicts the deployment of the BADGER system. When in use, the system is suspended from a refueling bridge hoist. The bridge and hoist are used to position the equipment in the horizontal plane for the purpose of moving BADGER over specific storage cells for testing. The areal density gage is lowered into and withdrawn from a specific fuel cell via the BADGER drive system. The drive system is comprised of a stepper motor, gearbox, and winch assembly that remotely raises and lowers the BADGER hardware. Also included on the drive platform is a shaft encoder, which provides a precise measure of the axial elevation of the BADGER hardware, and a load sensor which trips the drive motor, should a large load be applied to the system.

The BADGER hardware consists of aluminum source and detector probe heads that are suspended by a set of stainless steel suspension poles. Figure 2-1 also shows an axial cross-section of the source and detector heads positioned in two adjacent storage cells. The source and detector heads consist of aluminum boxes with chamfered lead-ins on the bottom edges. The chamfered lead-ins assist in guiding the device as it is inserted into the storage racks.

Figure 2-2 shows a conceptual lateral cross-section of the source and detector probe heads. The detector head contains an aluminum block mounted on one inside face of the head that houses three, two inch high BF_3 detectors. The aluminum block is shielded on all sides except for a two-inch window aligned with the detectors facing the source head. The detectors are encapsulated in watertight housings that are sealed and are attached to waterproof detector cables. The source head contains a watertight aluminum tube which houses a ^{252}Cf source when the equipment is in use.

The underlying principle of BADGER operation is the attenuation of neutrons through the neutron absorber panel between the source and detectors. Pool water in the source head thermalizes a portion of the fission neutrons produced by the ^{252}Cf source. The number of thermal neutrons reaching the neutron detectors is a function of the number of boron-10 atoms (^{10}B areal density) in the neutron absorber panel between the source and detectors. The number of the detector counts, in turn, is a function of the ^{10}B areal density in the neutron absorber panels. For panels with high areal density, the detector counts are low, whereas for low areal densities, the counts are high. BADGER is calibrated by passing the source and detector heads through a calibration cell replicating rack conditions that contain sections of neutron absorber with known ^{10}B areal densities.

The detector signals are fed to three pre-amplifiers that are mounted on the drive assembly. Shielded cables connect the preamplifiers to three amplifiers/SCAs (single channel analyzer) in a Nuclear Instrument Module (NIM) bin positioned alongside the

pool. The NIM bin also houses two (2) high voltage power supplies used by the pre-amps. The amplified and modified detector signals are fed to a conversion box and then to a laptop computer for counting and recording. The computer serves as a data-logger and as a control unit for the drive system and load cell.

2.2 Typical Operation of BADGER

The BADGER system is applied to measure the ^{10}B areal density in spent fuel racks in the following sequence. First, the calibration cell is lowered into the pool, typically near the racks to be measured. After the equipment has been assembled poolside and suspended from the auxiliary crane, the ^{252}Cf source is transferred into the source tube, a seal plug is installed, and the source and detector heads are submerged in the pool.

The rack specific calibration cell has neutron absorber standards of varying known areal densities arranged axially, as well as gaps of known size. At the beginning of a test campaign, the BADGER probes are lowered into the calibration cell and the calibration cell is scanned. The bottom of the calibration cell establishes a reference elevation datum during calibration. After scanning of the calibration cell, BADGER is ready for test operations. Calibration scans at a minimum must be performed at the beginning and end of each test day.

The areal density of a Boraflex panel is determined by comparing the detector count rate through the panel to the count rates through panels of known areal density in the calibration cell. The absolute areal density in a panel is determined by constructing a fit of the form:

$$\rho_{AD} = m * \ln(TR) + b$$

Where: TR = neutron transmission
 ρ_{AD} = boron 10 areal density
 m = slope
 b = intercept with the ordinate

The slope and intercept of the curve in the above equation is determined by measuring the transmitted neutrons in the calibration cell over areas of known areal density. All statistical uncertainty is determined from natural counting uncertainty propagated over all data handling equations. Error propagation, where $f(x, \dots, z)$ is performed using the following equation.

$$\delta f = \sqrt{\left(\frac{\partial f}{\partial x} \delta x\right)^2 + \dots + \left(\frac{\partial f}{\partial z} \delta z\right)^2}$$

A Boraflex panel is tested in the following sequence. The probe is placed into two specific cells on either side of the Boraflex panel of interest and lowered to the bottom of

the cell. A load sensor on the lift assembly provides indication of when the probe is fully inserted. The reference elevation datum is established at the bottom of the cell and all measurements of probe elevation are relative to this datum.

The entire panel is scanned with the heads being moved in two-inch increments from the bottom of the cell to the top. The active portion of the detectors is two inches, so a scan measurement represents the entire panel. At each elevation, the counts of each detector are measured for a period of eight (8) seconds, and are recorded by the data-logging computer. As the scan proceeds, the test equipment operator monitors the computer as the counts for each detector are plotted on the screen as a function of axial elevation. The operator monitors the elevation data, alert to the fact that high count rates could be indicative of low boron-10 areal densities. After the neutron count rate versus elevation measurement is complete, the probes are moved out of the tested cells and to a new cell location for subsequent testing.

The process is repeated for all panels scheduled for testing. The total time required for a scanning measurement is typically about twenty minutes per panel. As data is recorded by the data logging computer, data files containing detector count rates versus axial elevation in the cells are created on the computer hard drive which serves as a permanent record of the measurements.

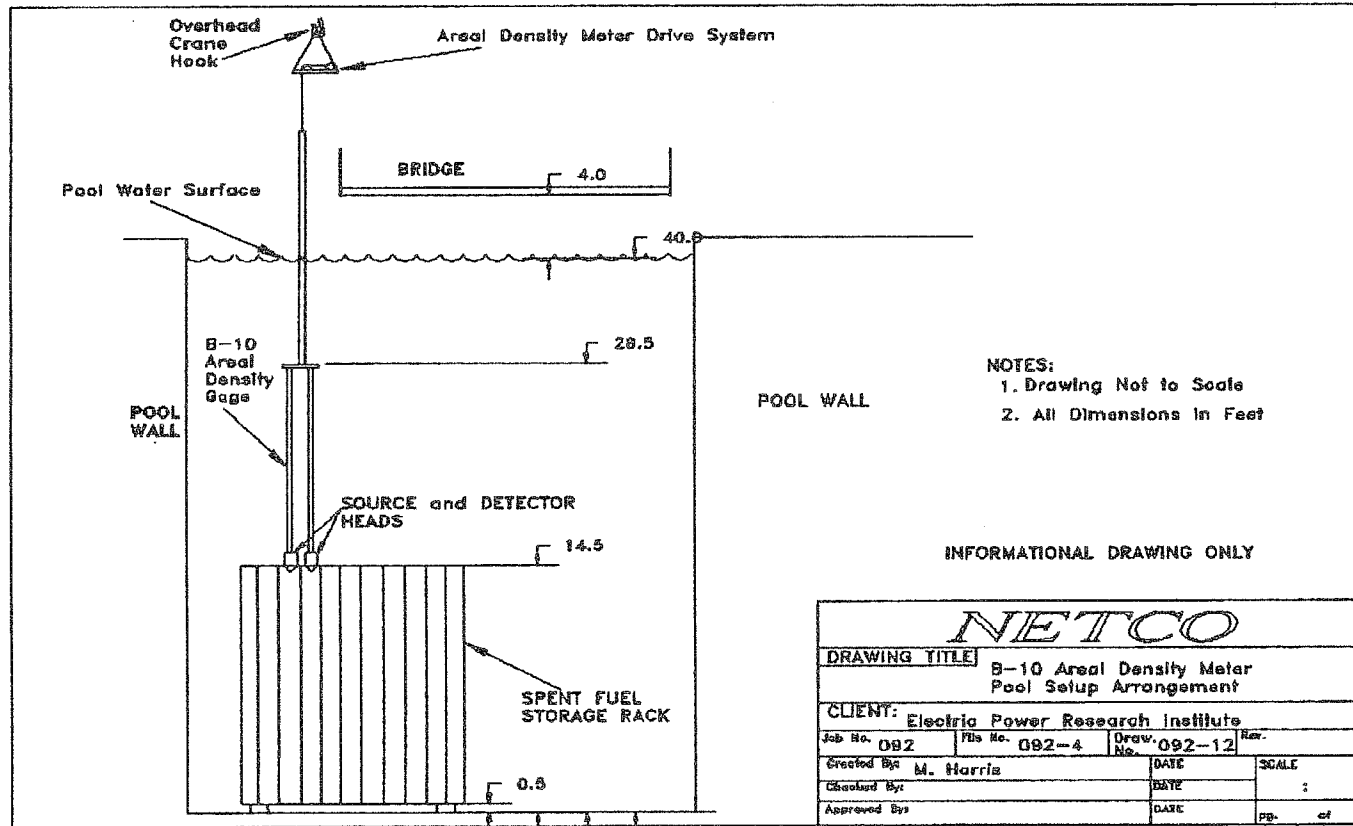


Figure 2-1
Typical Axial Cross Section of the Source and Detector Heads in Fuel Rack Cells

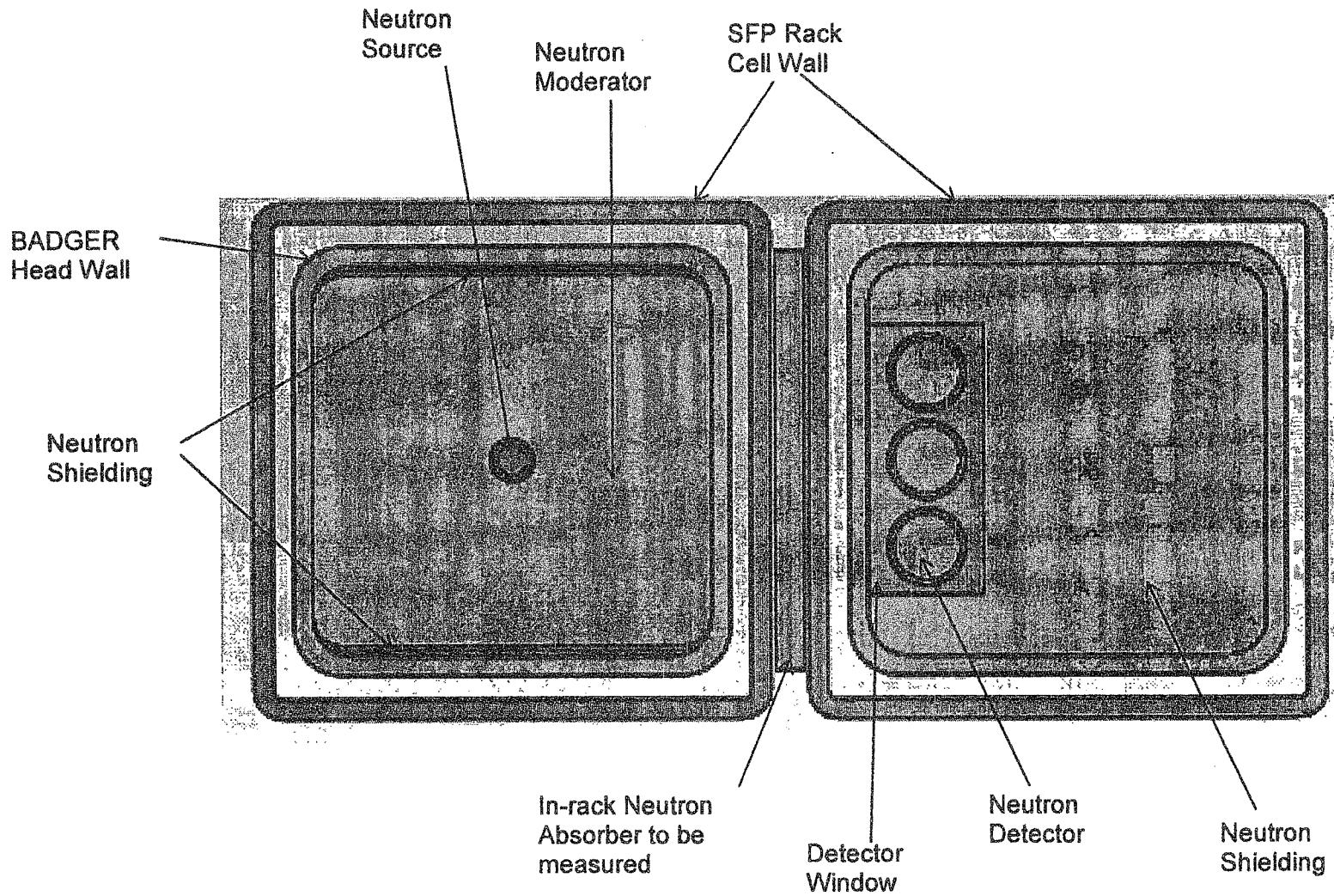


Figure 2-2
Lateral Cross Section of the Source and Detector Heads

3.0 SCOPE OF THE TESTING AT FERMI 2

3.1 *Spent Fuel Rack Description*

The spent fuel storage racks for the Fermi storage rack contain two types of absorbing material, BORAL[®] and Boraflex. The BORAL[®] racks were manufactured by Holtec and are not part of the scope of the BADGER testing. The Boraflex racks were fabricated by the Joseph Oat Corporation and are the center of the attention of this testing campaign.

The fabrication process started with the manufacture of a series of elements (hereafter designated by their form and noted as "Tee", "Ell", or "cruciform" shaped) which are subsequently welded together to form an "egg crate" structure which ultimately provides storage locations or cells for spent fuel assemblies. The basic Tee, Ell, and cruciform elements were manufactured by starting with Ell shaped sub-elements of stainless steel 6 inches on each wing, 175 inches long, and 0.075 inches thick as shown in Figure 3-1. A cavity for the Boraflex was created by using end strips of stainless steel to form a "picture frame" between adjacent Ell's as shown in Figure 3-2.

In the process used for manufacture, the strips forming the "picture frame" were tack welded to the stainless steel Ell's. To hold the Boraflex in place during manufacture, a Dow Silicon Adhesive (Dow No. 999) was used. A bead of adhesive was applied roughly to the center of the cavity and subsequently was distributed into a 2-1/2 inch to 3 inch wide strip along the entire axial length of the cavity with a stainless steel scraper. The Boraflex was then rolled into the cavity and pressed in place. The nominal dimensions of the Boraflex are 0.070 inches thick, 5.91 inches wide, and 152 inches in length. Fermi does not possess official documentation from the manufacturer stating the as manufactured areal density information. However, during the manufacturing process, individual batches of the Boraflex were tested for conformance with the minimum certified areal density. DTE Energy used these values to determine an average areal density and minimum areal density that was applied to their pool. This average value of 0.01662 g-¹⁰B/cm² and minimum value of 0.015656 g-¹⁰B/cm² are more representative of Fermi Unit 2's spent fuel pool than the manufacturing associated values. The 0.015656 g-¹⁰B/cm² minimum value will be the value to which the measured panels are ultimately compared.

To complete the rack module assembly, the structural elements containing Boraflex are welded together as shown in Figure 3-3. This rack design prevents, to a large extent, any interaction of the Boraflex with the pool water. This would, in theory, limit the dissolution of the Boraflex into the pool water.

3.2 Boraflex Panels Selected for Testing

A RACKLIFE model of the Fermi 2 racks and pool is updated and controlled by DTE Energy. The model was used to estimate the service history of each panel of Boraflex in the Fermi 2 storage racks, specifically estimated gamma exposure. The model included information regarding the predicted state of the spent fuel pool at the time of testing. Figure 3-4 provides the RACKLIFE predicted distribution of panel accumulated dose for the Fermi 2 spent fuel racks.

For the Fermi 2 spent fuel pool there is a large spread of dose across the pool. Near the transfer canal, the panel dose is relatively low, while the estimated dose of the east and north modules is much larger. The peak dose of a tested panel during the campaign is 1.67×10^{10} Rads. The selected panels test a variety of high dose and low dose panels. While the list of tested panels, Table 3-1, does feature some low dose panels, the test primarily focuses on the higher dose panels.

Integrated absorbed dose alone is not a sufficient predictor of panel boron carbide loss. Panels that received a moderate dose many years ago may have undergone more dissolution than panels that more recently received a higher dose. Once a critical dose level has been attained (about 2×10^9 rads), Boraflex becomes susceptible to dissolution by the pool water. Dissolution is an equilibrium reaction that is dependent upon the reactive silica concentration in the pool water. Dissolution is due to both the integrated dose above the critical value and the interaction of low silica concentration pool water with the high dose panel. Panel dissolution can be strongly dependent upon panel cavity volume, water exchange rates between the panel cavity, and the bulk pool volume.

Table 3-1
RACKLIFE-Estimated Dose for Fermi 2 Boraflex Panels Tested

<i>Panel ID</i>	<i>Estimated Dose [Rads]</i>	<i>Panel ID</i>	<i>Estimated Dose [Rads]</i>
B33E	7.99E+07	G34S	2.53E+09
B33S	5.55E+07	G34W	3.17E+09
C34E	2.23E+09	GG30S	9.15E+09
C34N	1.04E+09	JJ56E	9.65E+09
C34S	1.03E+09	JJ56N	1.09E+10
C34W	2.21E+09	JJ56S	1.28E+10
C36W	2.36E+09	JJ56W	9.93E+09
D35E	1.95E+09	JJ58E	1.11E+10
D35N	2.18E+09	JJ58N	1.20E+10
D35S	2.29E+09	JJ58S	1.09E+10
D35W	1.10E+09	JJ58W	1.08E+10
DD33N	1.67E+10	JJ60E	1.26E+10
E34E	2.35E+09	JJ60N	1.09E+10
E34N	2.09E+09	JJ60S	9.87E+09
E34S	1.27E+09	JJ60W	9.83E+09
E34W	1.23E+09	KK57E	1.38E+10
EE30N	9.29E+09	KK57N	1.01E+10
EE34W	1.62E+10	KK57S	1.27E+10
F33E	2.25E+09	KK57W	1.39E+10
F33N	2.88E+09	KK59E	1.40E+10
F33S	1.38E+09	KK59N	9.62E+09
F33W	1.50E+09	KK59S	1.29E+10
F35E	2.18E+09	KK59W	1.37E+10
F35N	3.07E+09	KK61E	1.03E+10
F35S	2.43E+09	KK61S	1.32E+10
F35W	2.17E+09	KK61W	1.15E+10
FF29E	6.69E+09	PP64S	7.42E+09
FF31W	8.04E+09	PP64W	5.54E+09
G34E	3.44E+09	QQ64S	6.70E+09
G34N	2.90E+09	QQ64W	8.77E+09

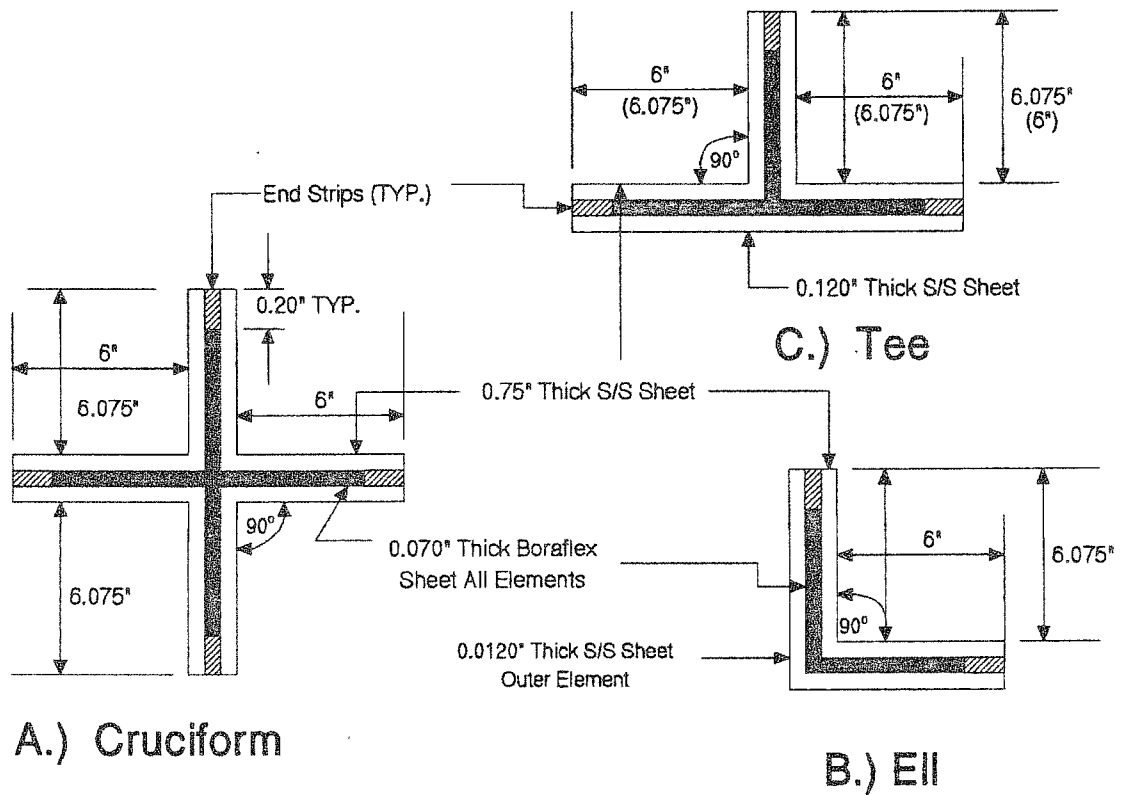


Figure 3-1
Fuel Rack Boraflex Configurations

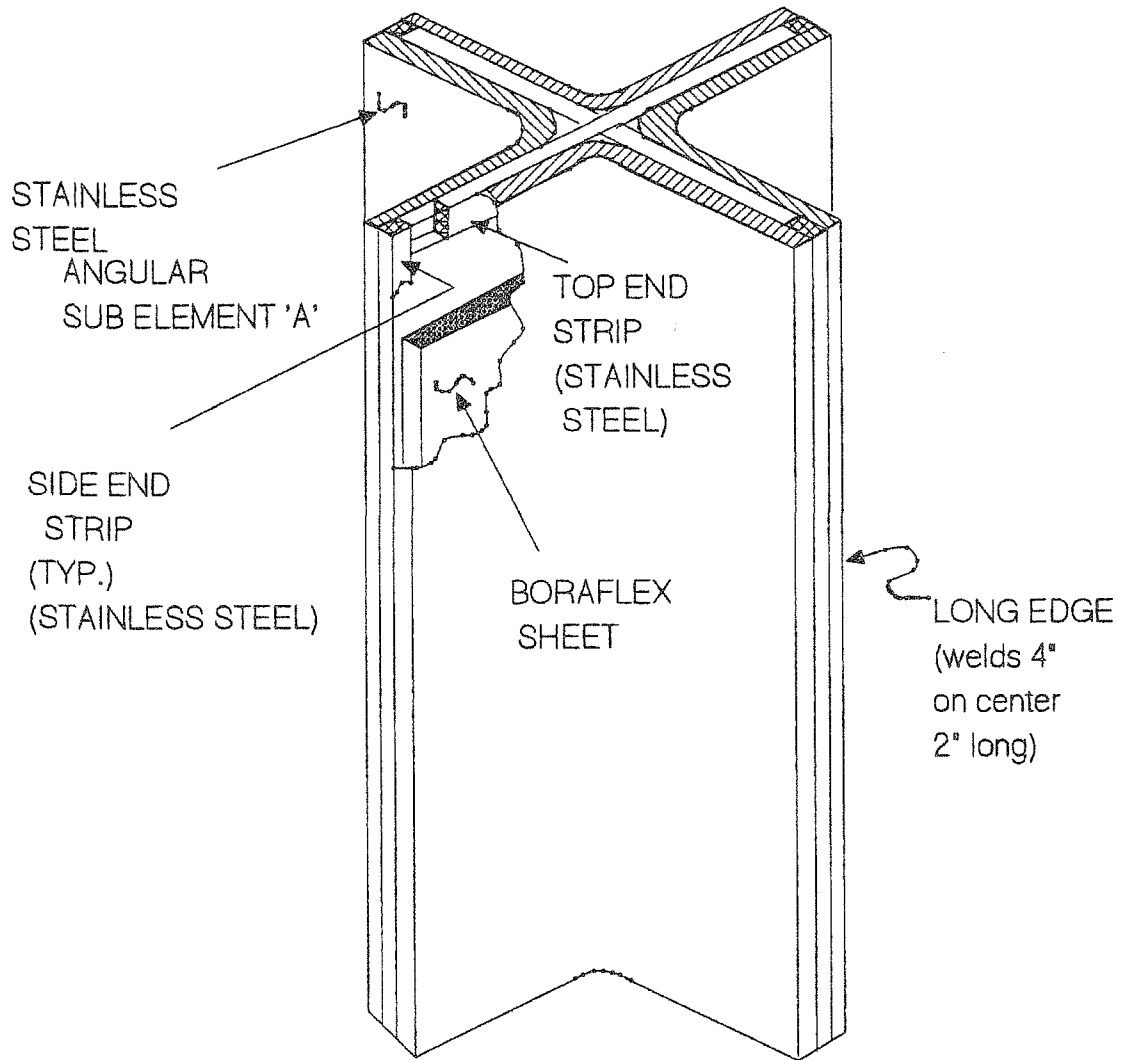


Figure 3-2
Isometric View of Cruciform Element

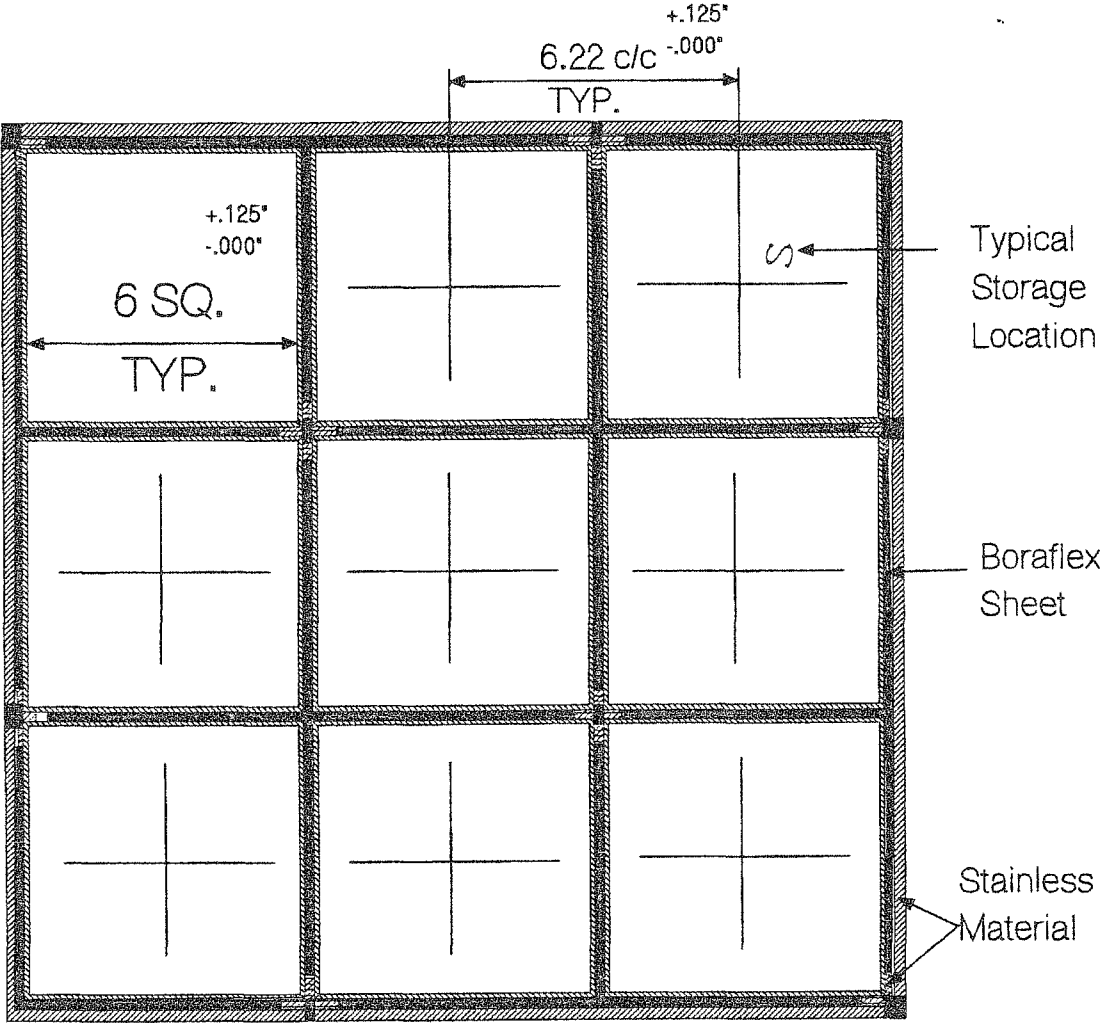


Figure 3-3
A 3x3 Array of Fuel Cells

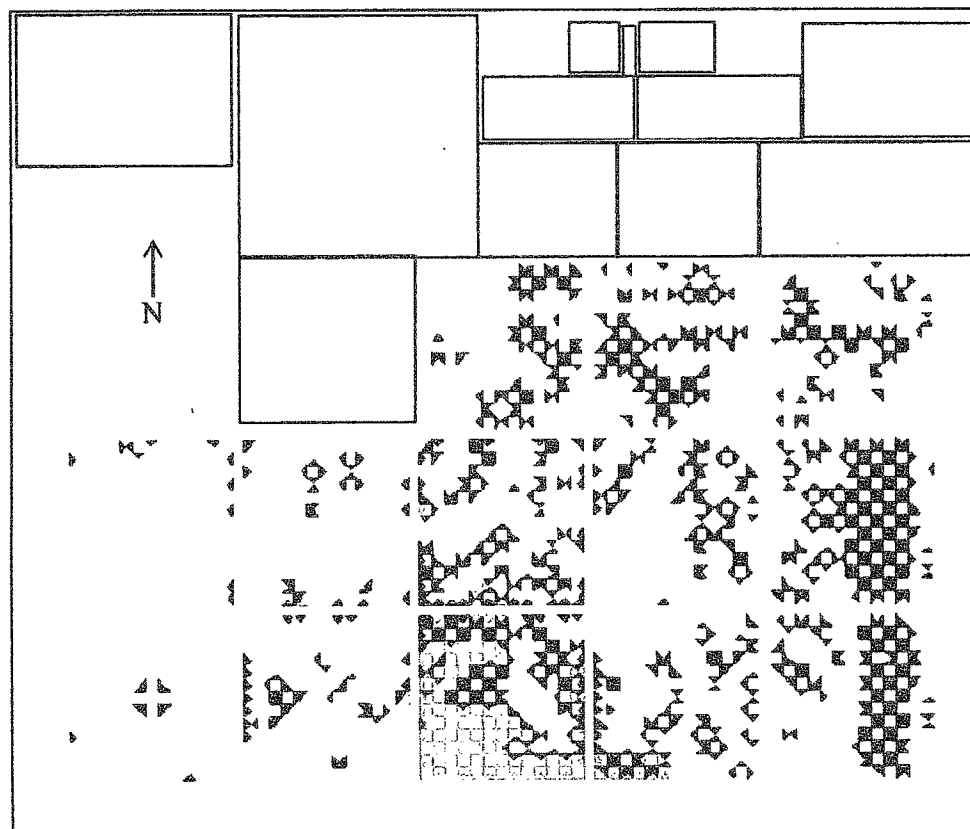


Figure 3-4
Distribution of (Estimated) Panel Dose in the Fermi 2 Spent Fuel Pool

Red is $\geq 1.0 \cdot 10^{10}$ rads
Yellow is $\geq 2.0 \cdot 10^9$ rads
Green is $\geq 5.0 \cdot 10^8$ rads
Blue is $< 5.0 \cdot 10^8$ rads

4.0 BADGER TEST RESULTS

4.1 Panel Detector Traces

The panel detector traces for all panels tested are contained in Appendix A. A panel detector trace is simply a plot of the received counts for each detector at each elevation. These panel traces provide insight into the panel condition and indicate gaps, local dissolution, or shrinkage. Thus, deviations from the flat trace represent shrinkage induced gaps, local dissolutions, local differences from a uniform panel, boron carbide loss or a combination thereof. A flat trace is not indicative of zero dissolution, only that the panel is uniform. The relevant features of a few of these panel traces are described below as an aid in interpreting the traces in Appendix A. It should be noted that when referring to dose below, that it is referring to the integrated gamma dose absorbed by the Boraflex panels.

Figure 4-1 contains a plot of the detector traces for the scan of panel B33 South. B33 South is the lowest dose panel of the panels that were tested with an estimated accrued dose of 5.55×10^7 Rads. This dose is low enough that the panel should not show significant effects of shrinking. An examination of Figure 4-1 indicates that B33 South shows an even and smooth scan with a clearly defined unattenuated region above the panel. This is indicative of an intact satisfactory panel.

Figure 4-2 contains a plot of the detector traces for the scan of panel KK57 West. The RACKLIFE estimated dose of the panel is high at 1.39×10^{10} Rads, which should show effects of shrinking, densification and possibly dissolution of the matrix. An examination of Figure 4-2 clearly shows a large gap near the 140" elevation, which is at least 4" in size. The rest of the panel appears to be intact with an exception of some local dissolution from the 10"-20" elevations. This is a clear example of a single large gap of expected size. This degradation is typical of a Boraflex panel at this level of gamma dose.

Figure 4-3 contains a plot of the detector traces for the scan of panel QQ64 South. The RACKLIFE estimated dose of the panel is 6.70×10^9 Rads. Shrinkage simulations indicate that panels receiving this amount of dose can be subject to several inches of gaps. This panel does not show any definitive gaps, but there is a section from 70"-80" elevation that shows significant degradation. The shape of the trace in this region is not indicative of a gap, so the result is most likely local dissolution.

Figure 4-4 contains a plot of the detector traces for the scan of panel JJ56 South. The RACKLIFE estimated dose of the panel is 1.28×10^{10} Rads. This dose is high enough to start the dissolution of Boraflex in pool water and show several inches of gaps. This panel shows both an area of dissolution in the 0"-40" elevation range and a large gap near the 130" elevation. Both of these features are expected in Boraflex with an absorbed dose over 10^9 Rads.

4.2 Panel Average Areal Density

As described in Section 3.1, DTE Energy adopted the results of the manufacturer sample tests and from those tests derived a representative average areal density value and an associated minimum areal density value. The derived average is $0.0166 \text{ g}^{-10}\text{B}/\text{cm}^2$ and the minimum value is $0.015656 \text{ g}^{-10}\text{B}/\text{cm}^2$. These areal density values are representative of the Boraflex in Fermi Unit 2's spent fuel pool. The $0.015656 \text{ g}^{-10}\text{B}/\text{cm}^2$ minimum value will be the value that the BADGER measured panels are ultimately compared to, due to its use in Fermi 2's Criticality Safety Analysis (CSA).

Table 4-1 contains the list of the sixty (60) tested panels from the 2013 Fermi Unit 2 BADGER Campaign and the corresponding calculated areal density values. The listed values in Table 4-1 are estimated dose, intact panel average areal density, uncertainty (2σ), intact panel minimum areal density, and gap values. In Table 4-1 the average panel areal density is reported as the "intact panel average areal density." The regions of the panel which are devoid of gaps or local dissolution are referred to as the intact regions.

The intact panel average areal density reported in Table 4-1 is determined as follows. An areal density value is calculated for all "intact" portions of the panel. That means an areal density value is calculated for each elevation that does not give indication of local degradation. This "intact" region of the panel includes and accounts for uniform thinning of the panels. The average areal density value is the average of the areal density values calculated at each "intact" elevation. The areal density calculation performed at each elevation is described in Section 2.2.

In Table 4-1 the minimum areal density column represents the 95/95 minimum areal density value. The 95/95 minimum areal density value is the minimum value calculated per NUREG/CR-6698 guidance. For added conservatism, it is assumed that the data for each panel is not normally distributed. Per NUREG/CR-6698, if the data is not normally distributed *and* there are at least 59 samples, then when the data (areal density values in this case) is ranked the lowest value becomes the one sided 95/95 minimum value.

The uncertainty values used in these cases are the calculational uncertainties in the areal density measurement, as described by in Section 2.2 at each elevation specific areal density. The uncertainty for the overall panel is determined conservatively by choosing the highest elevation specific uncertainty over the entire panel length. These uncertainty values in Table 4-1 are reported at the two sigma level. There are nine panels due to the presence of gaps for which fewer than 59 intact elevation-specific areal density values were calculated. In these cases, the minimum areal density value is conservatively calculated by taking the three sigma calculated uncertainty and subtracting it from the average areal density value (designated by **). The three sigma calculated areal density uncertainty is calculated by multiplying the two sigma

uncertainty by 3/2. This approach helps ensure that the randomness of the Boraflex degradation behavior is captured.

Values of average and minimum areal density as well as uncertainty are calculated for all three detectors; however the values reported in Table 4-1 are for the center detector. The center detector was chosen because the two outer detectors are influenced by neutrons that scatter around the neutron absorber panel. These scattered neutrons falsely lower the measured areal density value.

The average intact panel areal density of all panels measured is $0.0182 \text{ g}^{-10}\text{B}/\text{cm}^2$. This is significantly higher than the as-manufactured value of the areal density limit as stated above. The two sigma standard deviation in the spread of the panel areal densities is $0.0014 \text{ g}^{-10}\text{B}/\text{cm}^2$. The lowest intact panel average areal density value of all the panels tested is $0.0169 \text{ g}^{-10}\text{B}/\text{cm}^2$.

The plotted data in Figures 4-5 and 4-6 represents the areal density results displayed in Table 4-1. In Figure 4-5 the areal density is plotted versus the alphabetically ranked panel ID for each rack location. This means that the areal densities of panels from the same regions are plotted in close proximity of one another. This plot shows that the areal density values do not show a trend based on location. In Figure 4-6 the areal density values are ranked in order from lowest to highest. This plot shows that the data is evenly distributed around the $0.0182 \text{ g}^{-10}\text{B}/\text{cm}^2$ average. This plot also reinforces that there is a relatively small spread in the average intact areal density values among the panels.

In Figure 4-7 the areal density vs. the estimated panel dose as represented in Table 4-1 for all panels tested is plotted. This plot does not show a clear correlation between panel average intact areal density and associated estimated gamma dose. As can be observed, there are panels with high dose and high areal density and there are panels with low dose and low areal densities. The test does not appear to indicate an areal density versus RACKLIFE estimated gamma dose trend.

The average areal density of $0.0182 \text{ g}^{-10}\text{B}/\text{cm}^2$ is higher than the values adopted by DTE Energy. As stated previously, the values assumed by DTE Energy are significantly lower than the as manufactured values. The major reason that the measured values are higher than nominal values is due to the gamma induced polymer cross linkage which results in the densification of the panels. Densification increases the areal density upwards of 10% above the original value. This would bring the calculated values in close proximity to the DTE Energy adopted nominal value.

4.3 Gaps, Cracks, and Other Anomalies

Boraflex is predisposed to forming gaps due to radiation-induced shrinkage. Shrinkage can be accentuated by the non-uniform nature of the gamma dose absorbed by a Boraflex panel in the spent fuel pool racks. Absorbed dose gradients across and along a panel will cause differential shrinkage, which leads to shear stresses. This process is enhanced by the tendency of Boraflex to swell and to harden more rapidly under conditions when water from the aqueous pool environment more rapidly ingresses into the panel cavity, such as between welds or where there are manufacturing anomalies that permit increased flow into the panel cavity enclosure. The presence of these conditions results in shrinkage-induced gaps.

Table 4-1 includes two columns that characterize the gap formation in the panels. Cumulative Gap Size represents the sum of individual gap sizes over the entire panel. Every counting elevation that is not a part of the "intact" panel is assumed to have a gap. In actuality, these panel locations may either contain a gap or local dissolution. In this analysis when local dissolution is observed, a gap is assumed for conservatism. The sizes of the gaps are characterized using data from the associated calibration scan used for that panel. As documented in the Commercial Grade Dedication Plan, the Fermi 2 calibration cell has two gaps between the three (3) Boraflex standards. These gaps which effectively simulate actual gaps in Boraflex panels are 1" and 3" in size^[8]. Two separate linear fits are derived from the calibration cell scan data and applied to the assumed gaps. These estimated gaps are then summed along the length of the panel and reported in Table 4-1. The final column in Table 4-1, Uncertainty in Gap Size, lists the uncertainty in the reported gap value. The uncertainty is calculated on a per gap basis using propagation of error over all equations used. The total uncertainty is summed over the entire panel for each gap and is reported in Table 4-1.

In Figure 4-8 the estimated dose vs. gap size is plotted using values as represented in Table 4-1. This plot illustrates three important aspects of the link between gamma exposure and gap formation. The first is that there is a general trend for the amount of gapping in a panel to increase with increasing gamma dose. The second is that even if a panel has a relatively low estimated dose, the panel can still have a significant amount of cumulative gap size. Third and perhaps most importantly, though dose increases with gap size, it is still a random process. This is seen in the entire plot. There are multiple locations that show a very different degradation level, yet have the same dose. There are also panels with similar degradation and very different doses. This is confirmed by inspection of the Panel Traces in Appendix A. As stated in Section 3.2, panel dissolution can be dependent upon the time period in which dose was accumulated, amorphous silica concentration, panel cavity volume, water exchange rates between the panel cavity, and the bulk pool volume.

Figure 4-9 shows the number of panels that exhibit a certain range of cumulative gap sizes. This figure shows that, for all of the panels tested, the cumulative gap size was less than 6 inches. This is an important result because research has shown that

radiation induced shrinkage asymptotically approaches 4% of the panel length as gamma dose continues to increase^[3]. In regards to the Boraflex panels in the Fermi Unit 2 spent fuel storage racks, the gamma induced panel shrinkage would asymptotically approach six (6) inches.

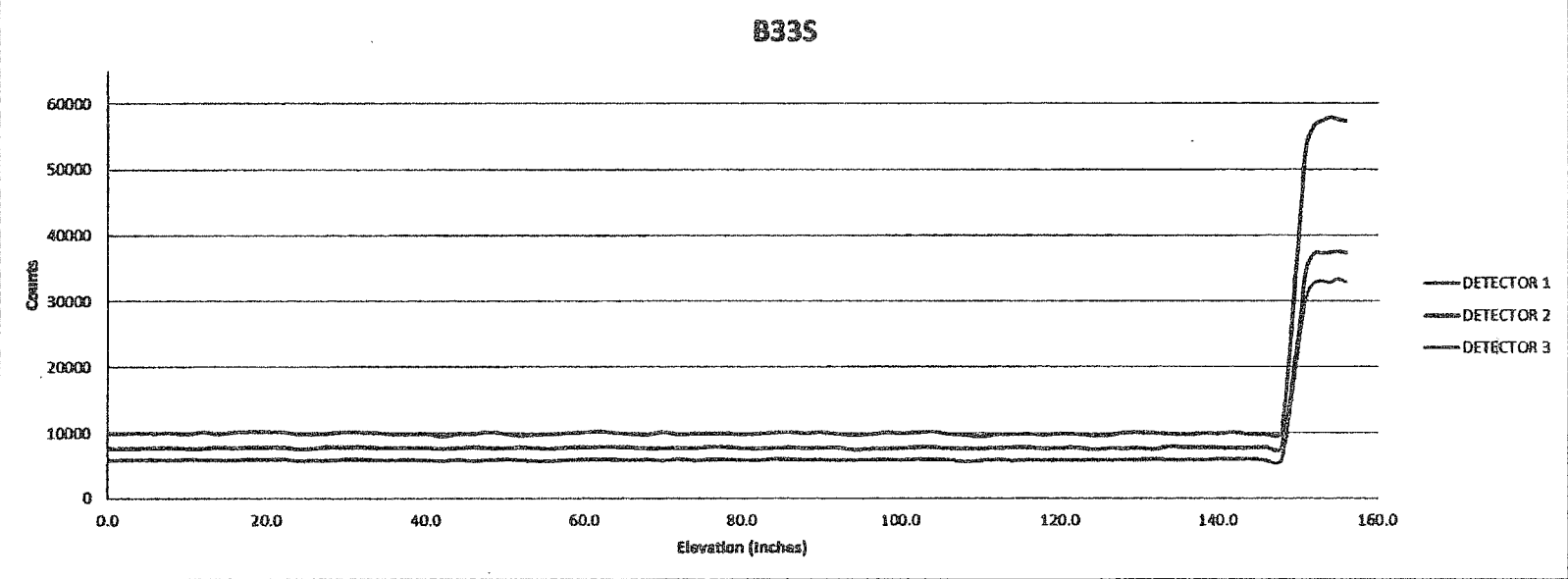


Figure 4-1
Panel Traces for Panel B33 South

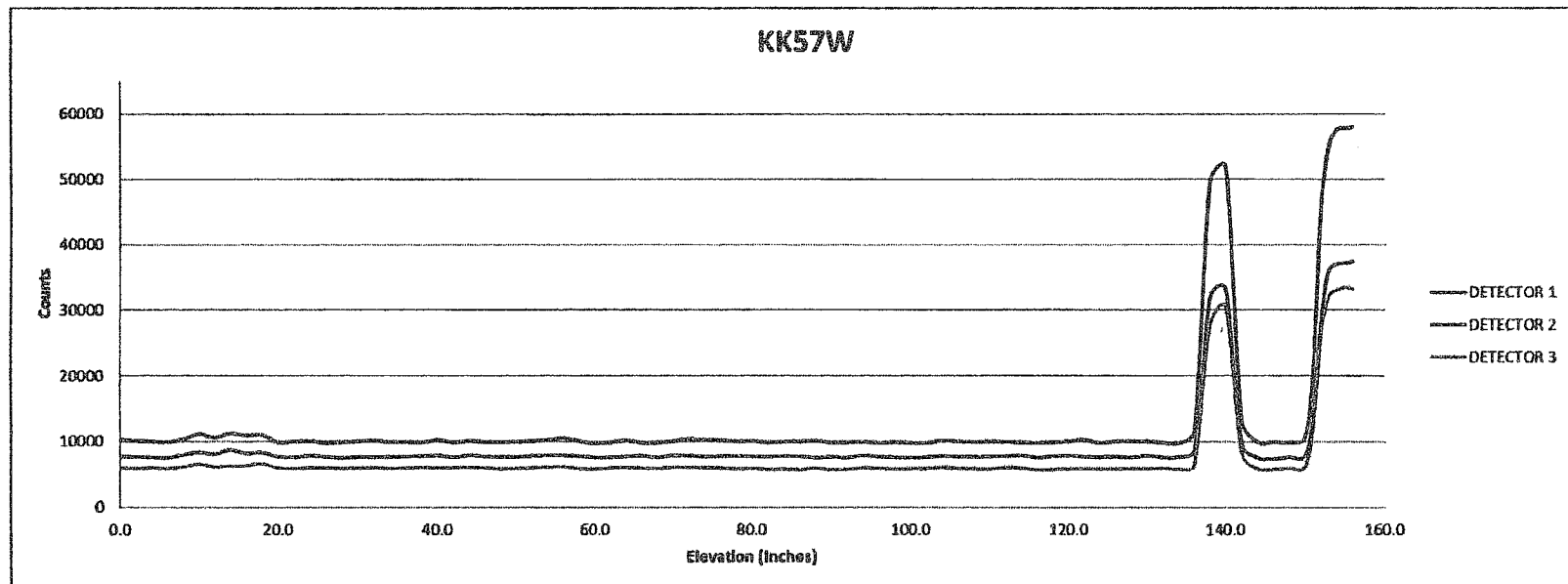


Figure 4-2
Panel Traces for Panel KK57 West. Features a Large Gap at 140".

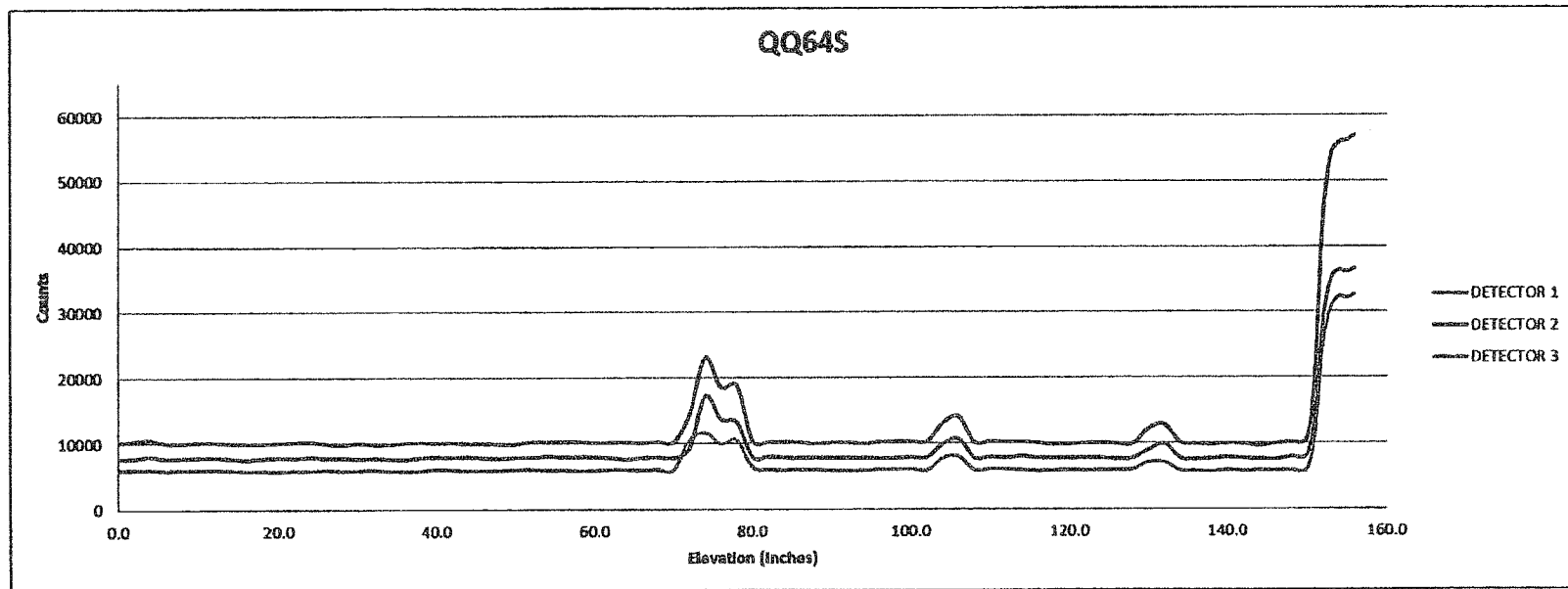


Figure 4-3
Panel Traces for Panel QQ64 South. Features a Local Dissolution from ~ 70" - ~ 80".

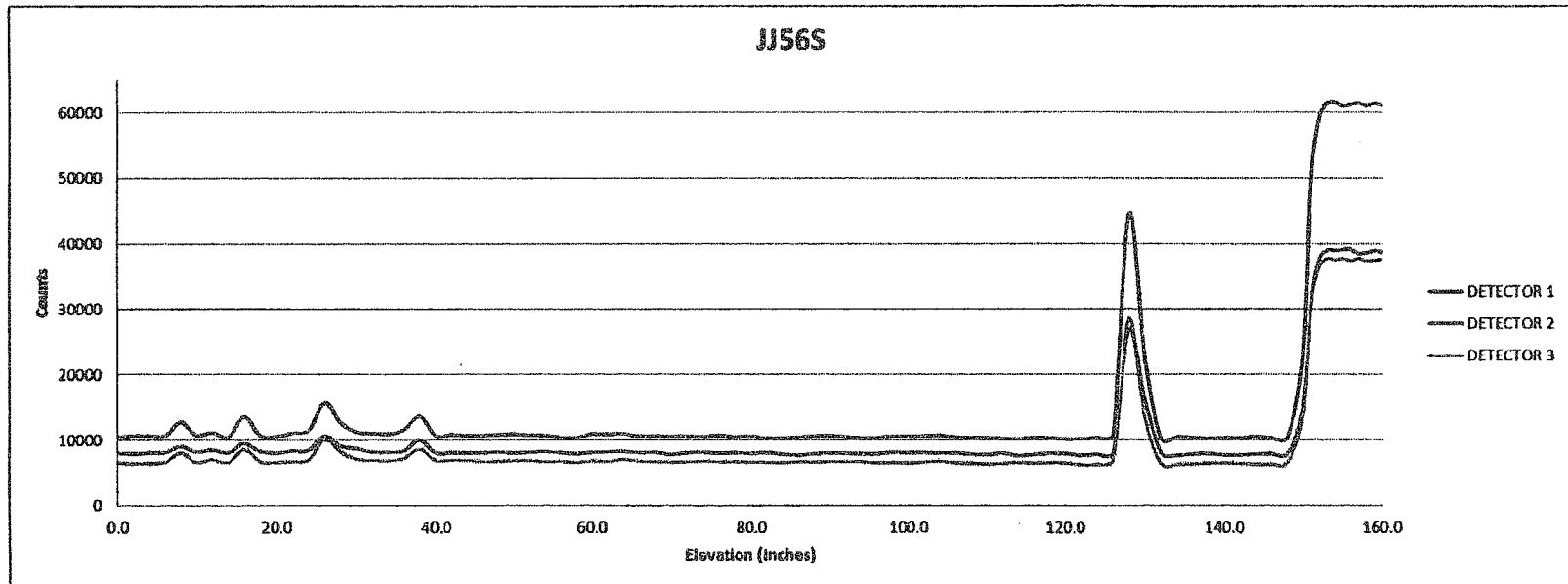


Figure 4-4
Panel Traces for Panel JJ56 South. Features a Large Gap at 130" and Local Dissolution from 0"-40".

Table 4-1
Fermi 2 Results for All Tested Boraflex Panels

Panel ID	Estimated Dose Value [Rads]	Intact Panel Average AD [$g^{-10}B/cm^2$]	Panel Average Uncertainty 2σ [$g^{-10}B/cm^2$]	Intact Panel Minimum AD [$g^{-10}B/cm^2$]	Intact Panel Maximum AD [$g^{-10}B/cm^2$]	Cumulative Gap Size [inches]	Uncertainty in Gap Size (2σ) [inches]
B33S	5.55E+07	0.0185	0.0013	0.0178	0.0194	0.0	0.0
B33E	7.99E+07	0.0174	0.0013	0.0168	0.0186	0.0	0.0
C34S	1.03E+09	0.0179	0.0013	0.0170	0.0193	0.6	0.7
C34N	1.04E+09	0.0180	0.0013	0.0174	0.0188	0.4	0.6
D35W	1.10E+09	0.0185	0.0013	0.0177	0.0191	0.6	0.4
E34W	1.23E+09	0.0176	0.0013	0.0168	0.0182	0.7	1.3
E34S	1.27E+09	0.0174	0.0013	0.0167	0.0184	0.2	0.9
F33S	1.38E+09	0.0171	0.0013	0.0160	0.0180	0.8	0.5
F33W	1.50E+09	0.0193	0.0014	0.0185	0.0209	0.8	0.6
D35E	1.95E+09	0.0173	0.0013	0.0169	0.0178	0.0	0.0
E34N	2.09E+09	0.0189	0.0013	0.0179	0.0196	0.1	0.3
F35W	2.17E+09	0.0187	0.0013	0.0180	0.0201	1.9	0.5
D35N	2.18E+09	0.0186	0.0013	0.0176	0.0194	0.0	0.1
F35E	2.18E+09	0.0169	0.0013	0.0150**	0.0175	1.3	2.8
C34W	2.21E+09	0.0179	0.0013	0.0172	0.0190	0.8	0.7
C34E	2.23E+09	0.0176	0.0013	0.0168	0.0184	0.2	0.4
F33E	2.25E+09	0.0181	0.0013	0.0168	0.0189	0.2	0.4
D35S	2.29E+09	0.0184	0.0013	0.0178	0.0192	1.1	0.6
E34E	2.35E+09	0.0170	0.0013	0.0156	0.0182	0.0	0.0
C36W	2.36E+09	0.0181	0.0013	0.0171	0.0188	1.1	0.9
F35S	2.43E+09	0.0181	0.0013	0.0173	0.0188	2.0	1.2
G34S	2.53E+09	0.0179	0.0013	0.0170	0.0188	0.8	1.9
F33N	2.88E+09	0.0185	0.0013	0.0171	0.0193	2.5	0.6
G34N	2.90E+09	0.0173	0.0013	0.0166	0.0181	0.2	1.0
F35N	3.07E+09	0.0179	0.0013	0.0160**	0.0184	1.7	2.8

Panel ID	Estimated Dose Value [Rads]	Intact Panel Average AD [$g^{-10}B/cm^2$]	Panel Average Uncertainty 2σ [$g^{-10}B/cm^2$]	Intact Panel Minimum AD [$g^{-10}B/cm^2$]	Intact Panel Maximum AD [$g^{-10}B/cm^2$]	Cumulative Gap Size [inches]	Uncertainty in Gap Size (2σ) [inches]
G34W	3.17E+09	0.0178	0.0013	0.0171	0.0185	0.1	0.4
G34E	3.44E+09	0.0181	0.0013	0.0167	0.0191	0.0	0.0
PP64W	5.54E+09	0.0182	0.0013	0.0176	0.0200	2.0	2.1
FF29E	6.69E+09	0.0180	0.0013	0.0172	0.0190	2.9	2.0
QQ64S	6.70E+09	0.0175	0.0013	0.0168	0.0184	2.1	1.3
PP64S	7.42E+09	0.0187	0.0013	0.0180	0.0196	3.4	2.0
FF31W	8.04E+09	0.0181	0.0013	0.0162**	0.0188	2.3	4.8
QQ64W	8.77E+09	0.0183	0.0013	0.0164**	0.0190	2.3	3.9
GG30S	9.15E+09	0.0169	0.0013	0.0150**	0.0180	3.0	3.6
EE30N	9.29E+09	0.0182	0.0013	0.0163**	0.0190	3.1	5.6
KK59N	9.62E+09	0.0176	0.0013	0.0170	0.0184	3.2	2.2
JJ56E	9.65E+09	0.0186	0.0013	0.0175	0.0199	3.0	1.6
JJ60W	9.83E+09	0.0182	0.0013	0.0173	0.0191	1.8	0.5
JJ60S	9.87E+09	0.0198	0.0013	0.0187	0.0206	3.3	1.9
JJ56W	9.93E+09	0.0179	0.0013	0.0171	0.0192	4.1	2.3
KK57N	1.01E+10	0.0177	0.0013	0.0167	0.0190	0.9	2.0
KK61E	1.03E+10	0.0187	0.0013	0.0180	0.0194	3.1	2.0
JJ58W	1.08E+10	0.0176	0.0013	0.0167	0.0186	0.0	0.2
JJ56N	1.09E+10	0.0190	0.0013	0.0181	0.0198	4.2	1.9
JJ58S	1.09E+10	0.0175	0.0013	0.0166	0.0185	0.8	1.7
JJ60N	1.09E+10	0.0203	0.0014	0.0190	0.0216	1.7	1.4
JJ58E	1.11E+10	0.0186	0.0013	0.0179	0.0196	4.4	1.9
KK61W	1.15E+10	0.0187	0.0013	0.0180	0.0199	1.0	0.7
JJ58N	1.20E+10	0.0188	0.0013	0.0177	0.0199	1.6	1.0
JJ60E	1.26E+10	0.0198	0.0014	0.0186	0.0212	2.1	1.6
KK57S	1.27E+10	0.0186	0.0013	0.0176	0.0196	0.9	0.7
JJ56S	1.28E+10	0.0188	0.0013	0.0180	0.0195	3.2	1.9
KK59S	1.29E+10	0.0185	0.0013	0.0179	0.0195	4.0	2.1

Panel ID	Estimated Dose Value [Rads]	Intact Panel Average AD [$g^{-10}B/cm^2$]	Panel Average Uncertainty 2σ [$g^{-10}B/cm^2$]	Intact Panel Minimum AD [$g^{-10}B/cm^2$]	Intact Panel Maximum AD [$g^{-10}B/cm^2$]	Cumulative Gap Size [inches]	Uncertainty in Gap Size (2σ) [inches]
KK61S	1.32E+10	0.0192	0.0013	0.0172**	0.0200	3.3	2.7
KK59W	1.37E+10	0.0177	0.0013	0.0158**	0.0188	1.9	3.5
KK57E	1.38E+10	0.0183	0.0013	0.0175	0.0203	4.5	1.9
KK57W	1.39E+10	0.0182	0.0013	0.0176	0.0187	4.5	2.3
KK59E	1.40E+10	0.0197	0.0014	0.0184	0.0211	1.9	1.1
EE34W	1.62E+10	0.0177	0.0013	0.0158**	0.0185	3.7	3.1
DD33N	1.67E+10	0.0190	0.0013	0.0180	0.0205	3.7	1.2

**In accordance with NUREG/CR-6698, there must be >59 samples to use the ranking technique. These panels did not have enough elevation specific areal density values to have reported 95/95 minimum areal density value. In place of this, the minimum panel areal density is conservatively represented by subtracting the three (3) sigma uncertainty from the average areal density value. See Section 4.2 for details.

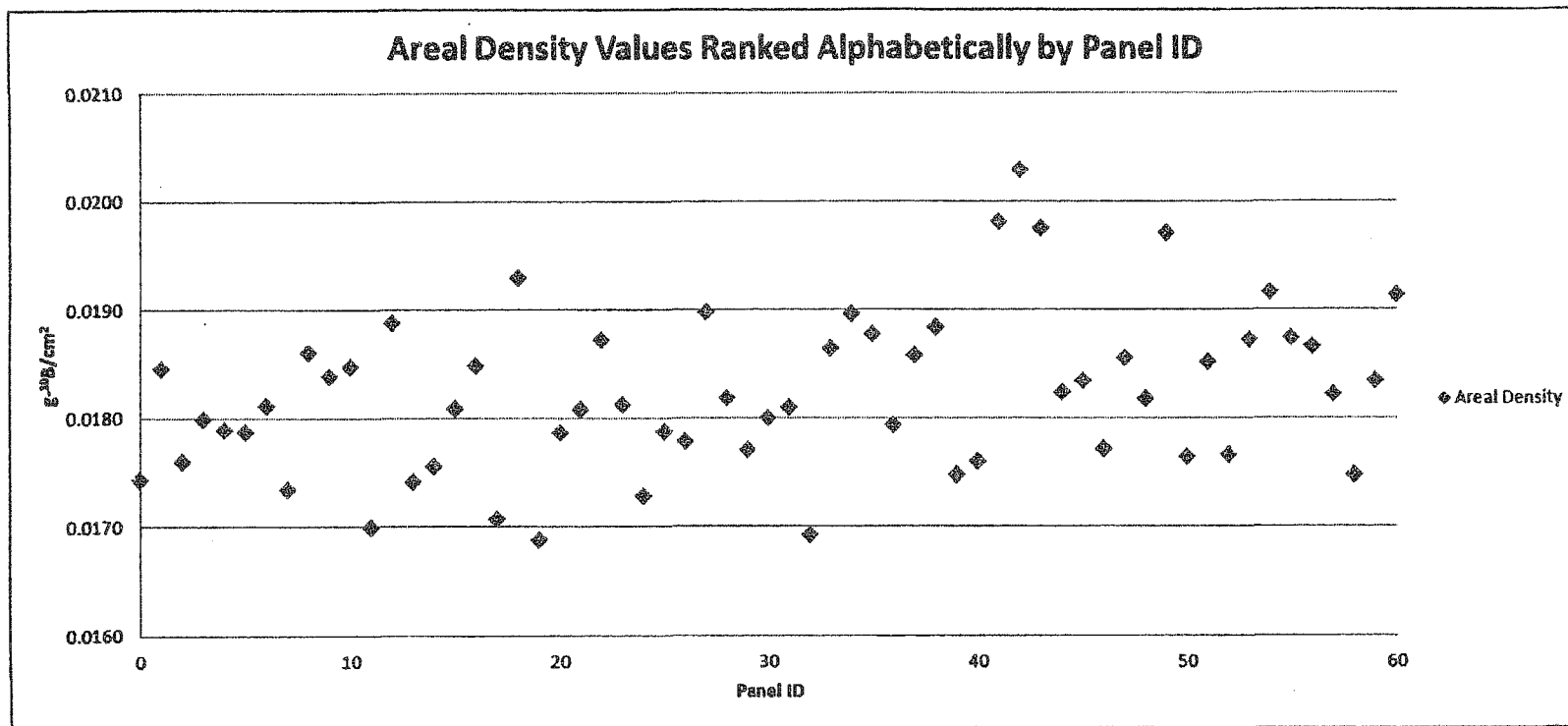


Figure 4-5
Distribution of Measured Areal Density Values Ranked Alphabetically by Panel ID for each rack location

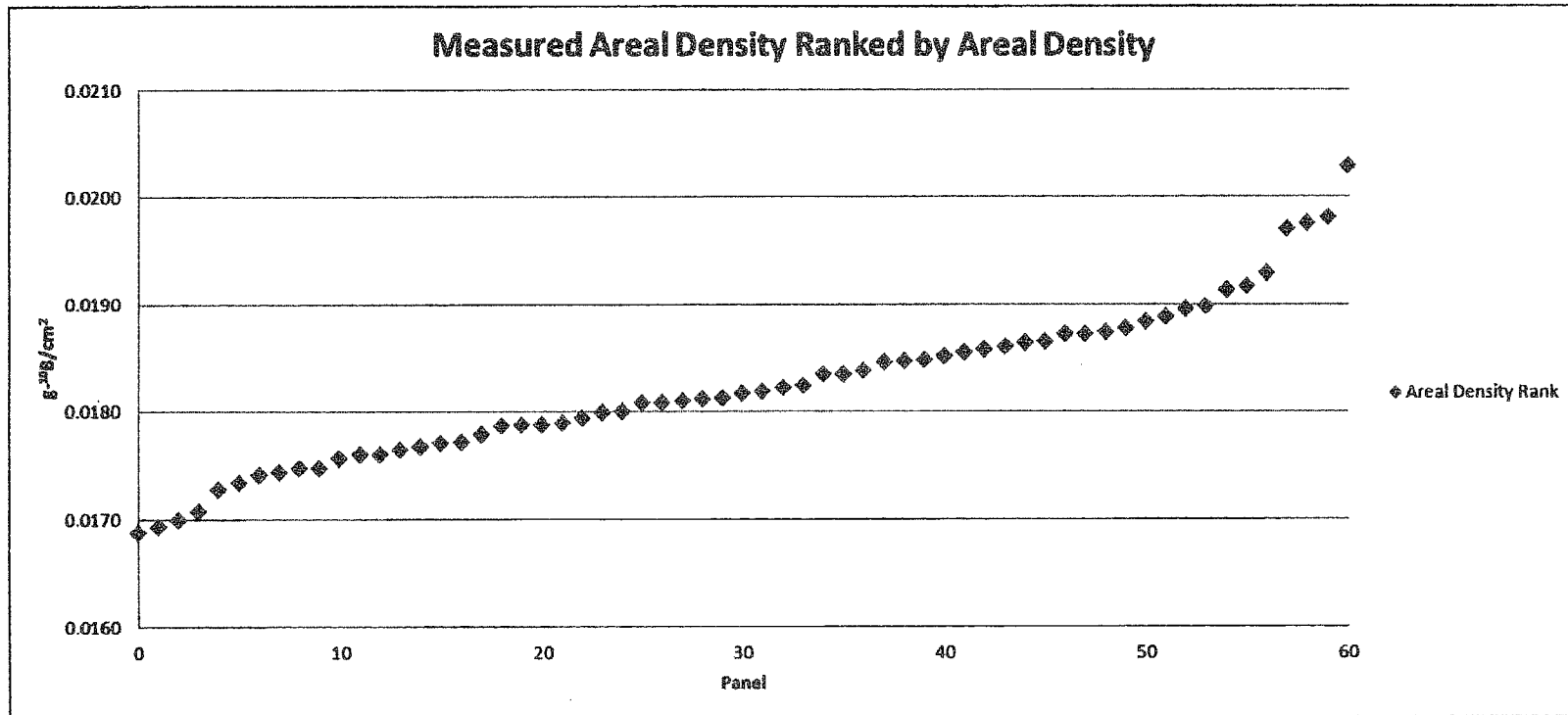


Figure 4-6
Distribution of Measured Areal Density Values Ranked by Areal Density

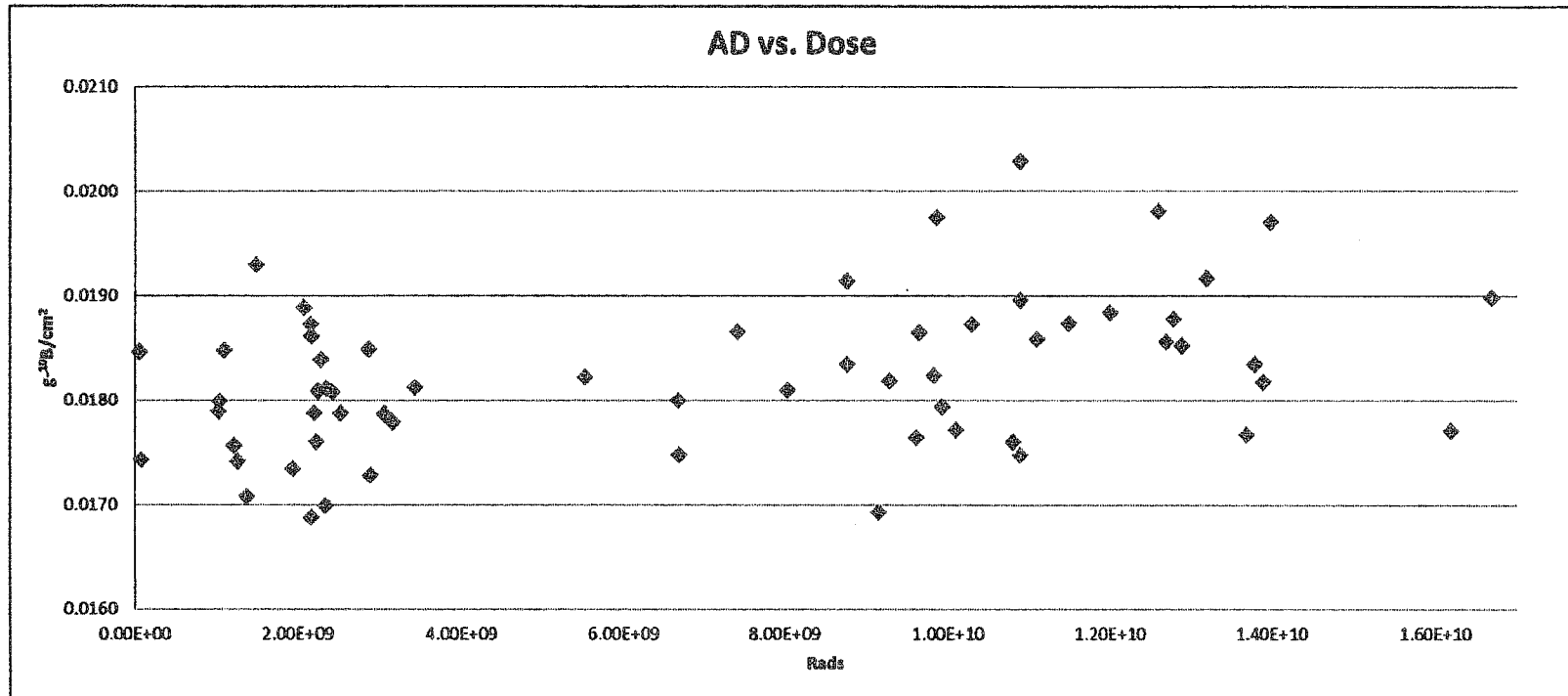


Figure 4-7
Distribution of Measured Areal Density (AD) Values versus the Estimated Dose as Predicted by RACKLIFE

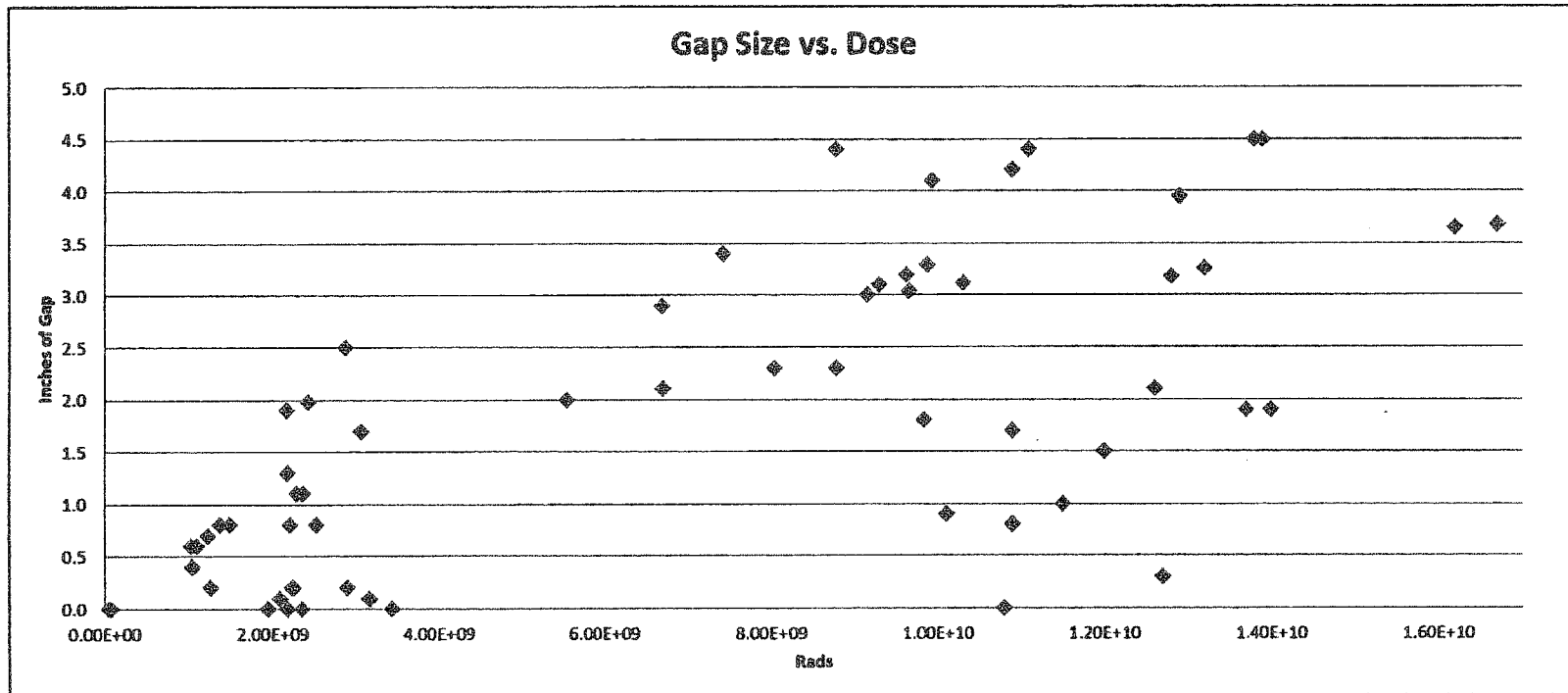


Figure 4-8
Distribution of the Cumulative Gap Size Observed on a Panel versus the Estimated Accumulated Dose as Predicted by RACKLIFE

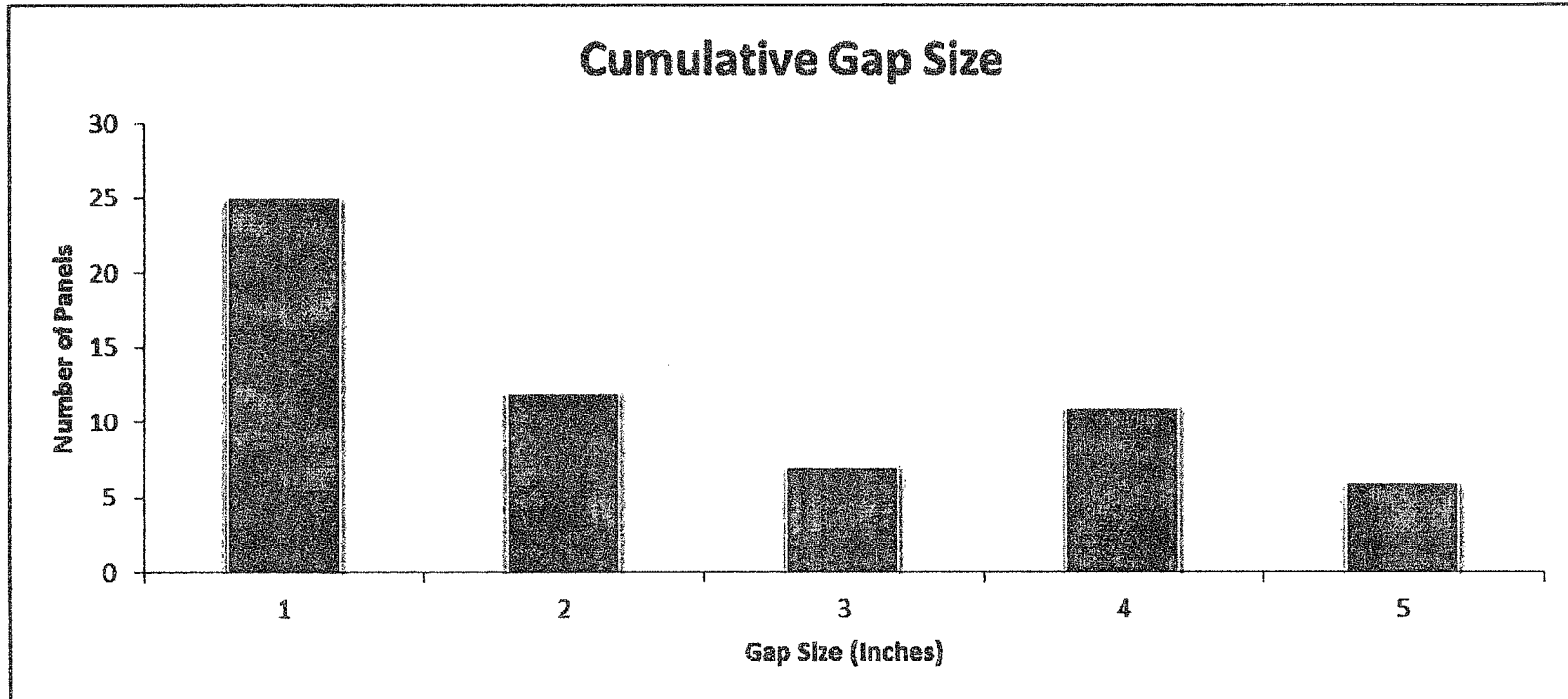


Figure 4-9
Histogram of the Number of Panels that have X" of Cumulative Gap Size

5.0 CONCLUSIONS

5.1 Test Results

A series of sixty (60) Boraflex panels from the Fermi 2 spent fuel racks have been subjected to non-destructive BADGER testing to determine the condition of the Boraflex neutron absorber material. The average areal density of all panels tested is $0.0182 \text{ g-}^{10}\text{B/cm}^2 \pm 0.0014 \text{ g-}^{10}\text{B/cm}^2$. The minimum areal density value limit, as stated previously, is the $0.015656 \text{ g-}^{10}\text{B/cm}^2$ value incorporated in the Fermi 2 spent fuel pool criticality analysis. There are three panels (E34E, F35E, and GG30S) that fall below this limit. These results and the gap results below should be compared to the criticality analysis to verify the acceptability of the condition of the Fermi 2 Boraflex panels.

For the panels tested, the results do not indicate extensive panel thinning; however, almost all of the tested panels exhibit some level of shrinkage induced gapping. As radiation dose increases, shrinking induced gaps are asymptotically limited to about 4% of the panel length. Consequently, the expected gap size should be limited to six (6) inches. No single gaps in excess of six (6) inches were observed. All panels showed cumulative gap sizes below six inches. If local dissolution were to occur in the vicinity of a gap, the effect would be to increase the gap size. The fact that observed cumulative gap size is thus far within the 4% limit associated with radioactive induced shrinkage tends to suggest that local dissolution is minimal.

DTE Energy performed blackness testing in 1992. The results of those tests indicated that for panel C36W there was a 1.08 inch gap at the 85 inch elevation.^[9] NETCO measured the same gap at the 80" elevation to be 0.8" with ± 0.3 " of uncertainty at the two sigma level. It can be concluded that within the reported level of uncertainty, the gap size has not changed since the 1992 blackness test.

When BADGER determined values of areal density are compared with nominal values, the Boraflex panels in Fermi 2's spent fuel pool storage racks shows evidence of satisfactory performance. In addition to the intact portion of the panel having sufficient reactivity hold down, the gaps that have been observed in the panels are of expected size and quantities for panels that have received such high levels of dose.

It should be noted that while the Boraflex may show satisfactory performance at this time, the Boraflex will eventually degrade past the acceptable point. The two most important factors that influence this inevitability are dose received and time. According to RACKLIFE, many of the panels have received the critical dose of 2×10^9 ; therefore a majority of the Boraflex panels are susceptible to degradation in the near future. The critical factor affecting the condition of the Boraflex panels is time.

5.2 Recommendations

To help monitor the condition of the Boraflex in the pool, NETCO recommends performing a BADGER test at a set time interval. This will aid the monitoring efforts in three ways. First, BADGER will give insight into the current condition of the pool. Second, if a selection (or all of) the same panels from this testing campaign are again tested in the future, then trending can be developed. Comparison of the condition of the panels from the current and future tests will indicate how panel areal density values and gap sizes will change over time. Third, BADGER can be used in concurrence with RACKLIFE (and other inputs such as pool chemistry) to help determine overall Boraflex panel condition.

As stated above, Boraflex will degrade in time. Performing BADGER tests, coupon surveillance tests, monitoring chemistry, and monitoring the RACKLIFE program will help determine and generally predict the condition of the Boraflex panels. These techniques, although useful to monitor evolving panel condition, cannot be relied upon to impede or prevent further deterioration. It is therefore recommended that DTE Energy should immediately begin one of three possible options. The first option would be to increase the removal of fuel from the pool into casks so that the fuel in the Boraflex racks can be safely stored without taking credit for Boraflex. The second option would be to remove the current Boraflex racks and replace them with new spent fuel pool racks. The third option would be to replace the neutron absorbing capabilities of the Boraflex material in the form of rack inserts. NETCO recommends these techniques to mitigate the decreasing reactivity hold down because, as stated above, Boraflex will dissolve and ultimately degrade below acceptable limits. DTE Energy should plan and be ready to mitigate the Boraflex issue before excessive degradation is discovered.

6.0 REFERENCES

1. White Paper: "Boraflex Performance in Spent-Nuclear-Fuel Storage Racks", Electric Power Research Institute: Palo Alto, California; August 1996.
2. "Radiation Induced Changes in the Physical Properties of Boraflex™, a Neutron Absorber Material for Nuclear Applications", K. Lindquist, D. Kline, and R. Lambert, Journal of Nuclear Materials: Vol. 217, pp. 223-228; 1994.
3. "Boraflex Test Results and Evaluation", TR-101986, Electric Power Research Institute: Palo Alto, California; February 1993.
4. "BADGER, a Probe for Nondestructive Testing of Residual Boron-10 Absorber Density in Spent-Fuel Storage Racks: Development and Demonstration", TR-107335, Electric Power Research Institute: Palo Alto, California; October 1997.
5. "MCNP Validation of BADGER", GC-110539 Electric Power Research Institute: Palo Alto, California; May 1998.
6. "The RACKLIFE Boraflex Rack Life Extension Computer Code: Theory and Numerics", TR-107333, Electric Power Research Institute: Palo Alto, California; July 1997.
7. SEP-300010-05, Rev 0 "Procedure for Assembly of the Boron-10 Areal Density Meter and Testing of BORAFLEX in the Fermi Unit 2 Spent Fuel Pool", NETCO, Lake Katrine; NY. August 20, 2013.
8. NET-300010-CGDP, Rev 2 "Commercial Grade Dedication Plan for Fermi 2 BADGER Testing/Calibration Cell Boron Carbide Standards" NETCO. Lake Katrine, NY. October 18, 2011
9. Kirkland, Matthew. "BADGER Report Comments." Message to Spencer Feuerstein. 17 January 2014.
10. J.C. Dean, R.W. Tayloe, Jr. (Science Applications International Corporation), Guide for Validation of Nuclear Criticality Safety Computational Methodology. Division of Fuel Cycle Safety and Safeguards, Office of Nuclear Material Safety and Safeguards, U.S. Nuclear Regulatory Commission. January 2001. NUREG/CR-6698.

Appendix A
BADGER Panel Traces for Tested
Panels

